Toward Controllable Molecular Shuttles**

Pier-Lucio Anelli, Masumi Asakawa, Peter R. Ashton, Richard A. Bissell, Gilles Clavier, Romuald Górski, Angel E. Kaifer, Steven J. Langford, Gunter Mattersteig, Stephan Menzer, Douglas Philp, Alexandra M. Z. Slawin, Neil Spencer, J. Fraser Stoddart,* Malcolm S. Tolley, and David J. Williams

Abstract: A number of nanometer-scale molecular assemblies, based on rotaxane-type structures, have been synthesized by means of a template-directed strategy from simple building blocks that, on account of the molecular recognition arising from the noncovalent interactions between them, are able to self-assemble into potential molecular abacuses. In all the cases investigated, the π-electron-deficient tetracationic cyclophane cyclobis(paraquat-*p*-phenylene) is constrained mechanically around a dumbbell-shaped component consisting of a linear polyether chain intercepted by at least two, if not three, π-electron-rich units and terminated at each end by blocking groups or stoppers. The development of an approach toward constructing these molecular abacuses, in which the tetracationic cyclophane is able to shuttle back and forth with respect to the dumbbell-shaped component, begins with the self-assembly of a [2]rotaxane consisting of two hydroquinone rings symmetrically positioned within a polyether chain terminated by triisopropylsilyl ether blocking groups. In this first so-called molecular shuttle, the tetracationic cyclophane oscillates in a degenerate fashion between the two π-electron-rich hydroquinone rings. Replacement of one of the hydroquinone rings—or the insertion of another π-electron-rich ring system between the two hydroquinine rings—introduces the possibility of translational isomerism, a phenomenon that arises because of the different relative positions and populations of the tetracationic cyclophane with respect to the π-donor sites on the dumbbell-shaped component. In two subsequent [2]rotaxanes, one of the hydroquinone rings in the dumbbell-shaped component is replaced, first by a *p*-xylyl and then by an indole unit. Finally, a tetrathiafulvalene (TTF) unit is positioned between two hydroquinone rings in the dumbbell-shaped component. Spectroscopic and electrochemical investigations carried out on these first-generation molecular shuttles show that they could be developed as molecular switches.

Keywords
molecular devices · nanostructures · rotaxanes · self-assembly · translational isomerism

Introduction

The nanometer scale has been highlighted as the size regime in which functioning molecular devices are most likely to operate.[1] Two approaches to the construction of such devices have been identified. One is the so-called "top-down" approach, in which bulk atomic or molecular arrays are dismantled down to the nanometer scale: it has been employed for many years as a means of miniaturizing electronic components. The other may be termed a "bottom-up" approach to the construction of devices that function at the molecular level: it exploits the natural processes of self-assembly[2] and self-organization,[3] wherein relatively simple and abundant molecular subunits come together as a result of favorable noncovalent bonding interactions, to form supramolecular arrays and molecular assemblies, some of which display novel functions.[4–7]

In pursuing the "bottom-up" approach, it occurred to us that mechanically bonded molecules, in which one molecular component is able to move relative to another, may provide a means of effecting reversible and controlled switching between two states[8] at the molecular level. Specifically, we have chosen mechanically interlocked molecules[9–13] in the shape of the so-called catenanes and rotaxanes (Figure 1) and shown that they can be constructed using self-assembly processes based on the mutual recognition and interaction of π-electron-rich aromatic units, π-electron-deficient bipyridinium units, and

[*] Prof. J. F. Stoddart, Dr. M. Asakawa, Dr. R. A. Bissell, Dr. S. J. Langford, Dr. G. Mattersteig, Dr. D. Philp, Dr. N. Spencer, P. R. Ashton, G. Clavier, R. Górski, M. S. Tolley
School of Chemistry, University of Birmingham
Edgbaston, Birmingham B15 2TT (UK)
Fax: Int. code +(121)414-3531
Prof. A. E. Kaifer
Department of Chemistry, University of Miami
Coral Gables, Florida 33124 (USA)
Prof. D. J. Williams, Dr. S. Menzer, A. M. Z. Slawin
Department of Chemistry, Imperial College
South Kensington, London SW7 2AY (UK)
Fax: Int. code +(171)594-5804
Dr. P. L. Anelli
BRACCO, via Egidio Folli 50, 20134 Milano (Italy)
Fax: Int. code +(2)2641-0678

[**] "Molecular Meccano", Part 10: for Part 9 see P. R. Ashton, R. Ballardini, V. Balzani, M. Belohradsky, M. T. Gandolfi, D. Philp, L. Prodi, F. M. Raymo, M. V. Reddington, N. Spencer, J. F. Stoddart, M. Venturi, D. J. Williams, *J. Am. Chem. Soc.* **1996**, *118*, 4931–4951.

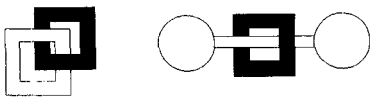

Figure 1. Schematic representations of a [2]catenane and a [2]rotaxane.

polyether chains. Of these two types of molecule, [2]rotaxanes[14] are more amenable to the development of a molecular switch. In chemical terms, this type of molecule contains a linear (*axle*) component encircled by a macrocyclic (*wheel*) component. To prevent the wheel from readily leaving the axle, the linear component must be terminated at both ends by large blocking groups or stoppers. The introduction of a variety of different recognition sites within the dumbbell-shaped component raises the possibility of multi-site occupancy by the macrocyclic component. Such a scenario could become the basis of a switching action if the preferred site of occupation—in a dissymmetric two-site system, for example—could be rendered responsive to an electronic, a photonic, or protonic stimulus. We describe here the synthesis, self-assembly, and physical properties of a range of [2]rotaxanes: **1**·4PF$_6$, **2**·4PF$_6$, **3**·4PF$_6$, and **4**·4PF$_6$, and their precursors and components (Figure 2). Some of the results discussed in this paper have been reported in preliminary form[15–18] and in a review.[19]

Results and Discussion

Preamble and Synthetic Strategy: The rotaxane-like orientations observed in the solid state[20] for the numerous 1:1 complexes formed between the tetracationic cyclophane[21] [BBIPYBIXYCY]$^{4+}$ and a range of different substrates led to the self-assembly of the first rotaxanes[11] in which two molecular components were mechanically linked by utilizing the two protocols (namely threading and clipping) already employed in the self-assembly of pseudorotaxanes.[22] When **5** was treated with triisopropylsilyltriflate in MeCN (Scheme 1) containing the cyclophane [BBIPYBIXYCY][PF$_6$]$_4$ and lutidine (with a threading protocol) the corresponding [2]rotaxane **6**·4PF$_6$ was isolated in 22% yield, following counterion exchange. The same [2]rotaxane **6**·4PF$_6$ (Scheme 1) can also be formed (from **7**, [BBIPYXY][PF$_6$]$_2$, and 1,4-bis(bromomethyl)xylene BBB) in 14% yield by employing the clipping protocol.[11] This first generation of [2]rotaxanes lacked the dynamic behavior of their [2]catenane counterparts.[11, 23] We soon recognized, therefore, that one way to impart to [2]rotaxanes a similar type of mechanical motion to that observed in those [2]catenanes was to introduce two recognition sites into the dumbbell-shaped component.

A. The First Molecular Shuttle: Our first approach to the design of a molecular shuttle (Scheme 2) involved the synthesis of a dumbbell-shaped compound containing two hydroquinone rings within a polyether chain terminated by two triisopropylsilyl ether blocking groups.[15] In essence, this dumbbell-shaped compound can be regarded as being formed by central scission of one of the polyether chains of BPP34C10 followed by the addition of the blocking groups (e.g., triisopropylsilyl ethers) to the primary hydroxyl group thus created (Figure 3). Hence, the design of this first prototype of a molecular shuttle can be related to {[2][BPP34C10]-[BBIPYBIXYCY]catenane}-{PF$_6$}$_4$. The dynamic properties of the [2]catenane (Figure 3) anticipate the shuttling process.[11]

Synthesis: The dumbbell-shaped component was synthesized in two steps from the readily available diphenol **8**,[24] which was bisalkylated (K_2CO_3/DMF) with **9** to afford the diol **10** (54%), which

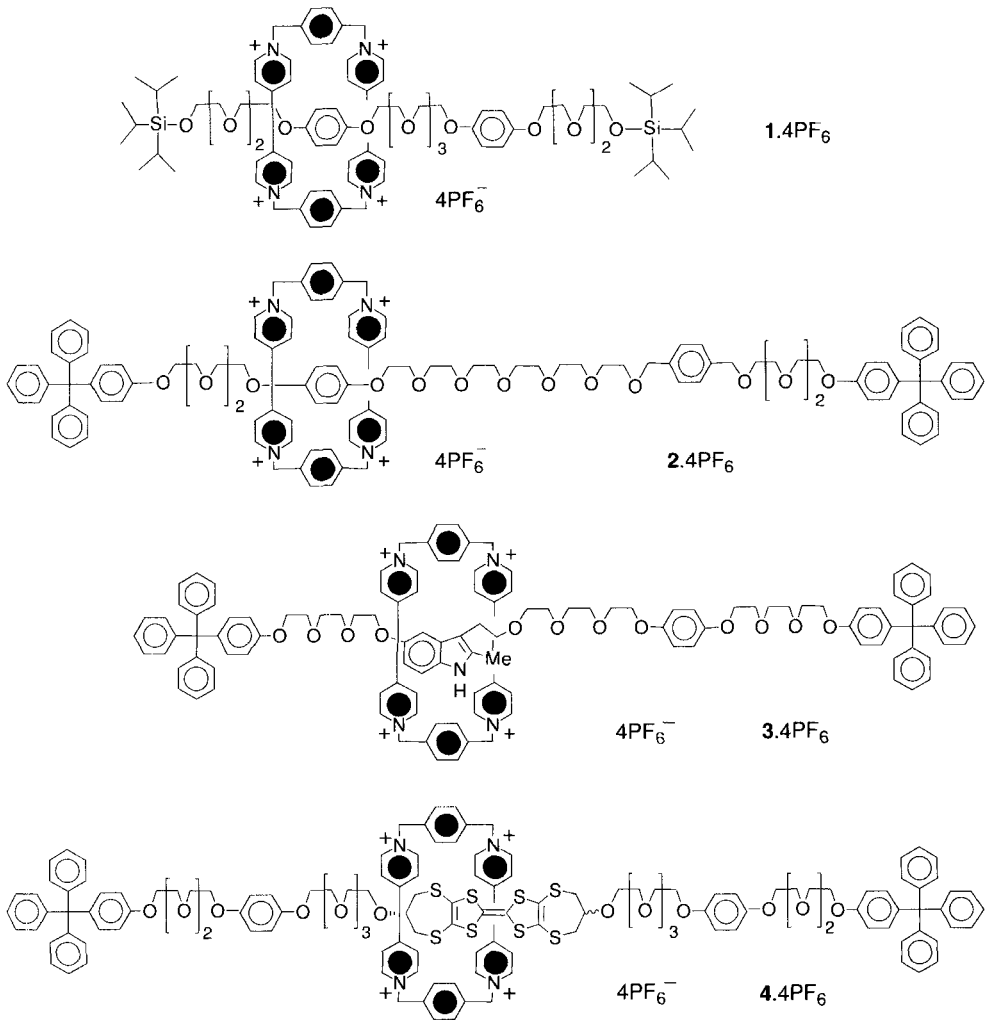

Figure 2. The molecular shuttles **1**·4PF$_6$ to **4**·4PF$_6$.

0947-6539/97/0307-1114 $ 17.50+.50/0 Chem. Eur. J. 1997, 3, No. 7

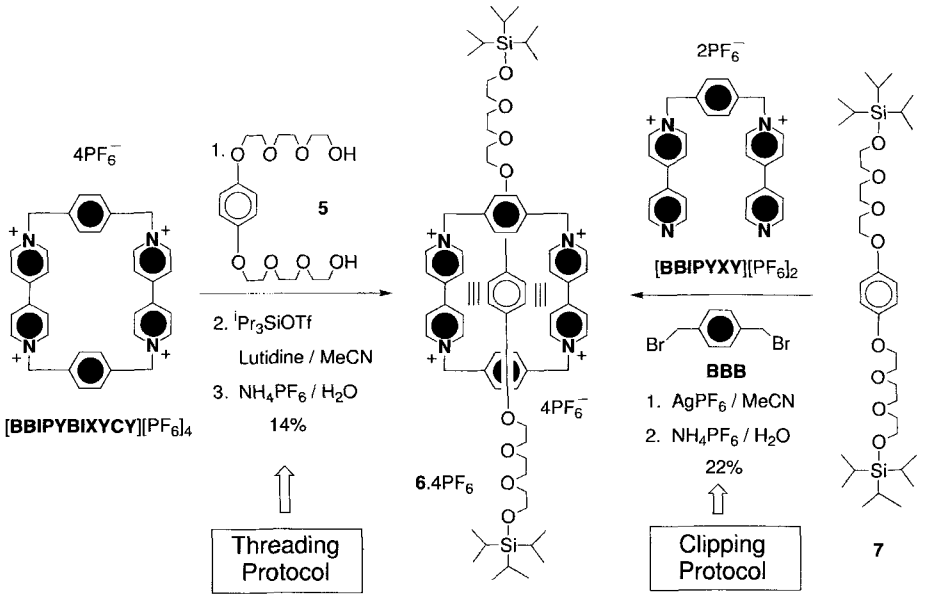

Scheme 1. Synthesis of [2]rotaxane $\mathbf{6}\cdot 4PF_6$.

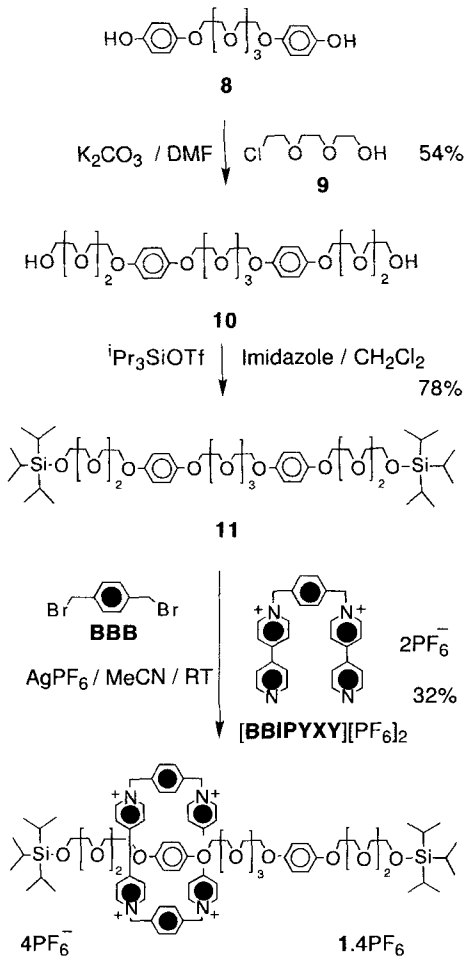

Scheme 2. Synthesis of [2]rotaxane $\mathbf{1}\cdot 4PF_6$.

was then converted by reaction (imidazole/CH_2Cl_2) with triisopropylsilyl triflate into the dumbbell-shaped compound **11** (78%). Under template-directing conditions, the reaction of $[BBIPYXY][PF_6]_2$ with BBB in the presence of **11** (3 molequiv) and $AgPF_6$ (2.5 molequiv)[25] in MeCN at room temperature gave the desired [2]rotaxane $\mathbf{1}\cdot 4PF_6$ as a deep orange-colored product in 32% yield (Scheme 2). This remarkably high yield is probably a consequence of the template-directing action of the two hydroquinone rings present in the dumbbell-shaped component during the cyclization of the tricationic intermediate that is presumably formed en route to the tetracationic cyclophane component of $\mathbf{1}\cdot 4PF_6$. Fast atom bombardment (FAB) mass spectrometry[26] and dynamic ^{1}H NMR spectroscopy were used to characterize this [2]rotaxane.

NMR Spectroscopy: Both the ^{1}H and ^{13}C NMR spectra of the [2]rotaxane $\mathbf{1}\cdot 4PF_6$ show temperature-dependent behavior in a range of deuterated solvents. In the ^{1}H NMR spectrum, we might expect to observe two sets of signals for the hydroquinone rings—one, possibly broad, set for the protons on the encircled hydroquinone ring, and a sharper AB-like system arising from the protons on the free hydroquinone ring. However, at room temperature in CD_3COCD_3 solution, a different situation is observed (Figure 4). The usually sharp signals corresponding to the OCH_2 protons are broad, while those for the hydroquinone ring protons are merged into the baseline between $\delta = 3.5$ and 6.5.[27] Clearly, at this temperature, the [2]rotaxane is experiencing a number of slow exchange processes on the ^{1}H NMR timescale. The position of the tetracationic cyclophane and hence its rate of shuttling between the two hydroquinone rings in the dumbbell-shaped component can be controlled by varying the temperature. Cooling the CD_3COCD_3 solution of $\mathbf{1}\cdot 4PF_6$ down to 223 K allowed a four-proton AA′BB′ system centered at $\delta = 6.38$ to be identified as arising from the free hydroquinone ring. Saturation transfer experiments under conditions of slow site exchange allowed us to identify a signal at ca. $\delta = 3.8$ for the protons belonging to the encircled hydroquinone ring, resonating under the signals for the OCH_2 protons. The distinction between encircled and free recognition sites implies that shuttling is slow at this temperature on the ^{1}H NMR timescale, a fact substantiated by the separation of signals for the triisopropyl groups on the silylated stoppers and for the α- and β-bipyridinium protons associated with the tetracationic cyclophane. The coalescence of the signals associated with these different ^{1}H NMR probes (Table 1) in both the dumbbell-shaped and tetracationic cyclophane components afforded the activation energy barrier ($\Delta G_c^{\ddagger}$) for the shuttling of the tetracationic cyclophane in $\mathbf{1}\cdot 4PF_6$ of ca. 13 kcal mol^{-1}. This value of $\Delta G_c^{\ddagger}$ is somewhat less than that for the corresponding circumrotation of BPP34C10 through the cavity of the tetracationic cyclophane in the [2]catenane shown in Figure 3.[11] When the same sample is warmed up to 413 K in CD_3SOCD_3, an eight-proton AA′BB′ system centered at $\delta = 5.16$ can be identified as arising from the hydroquinone protons. At this temperature,

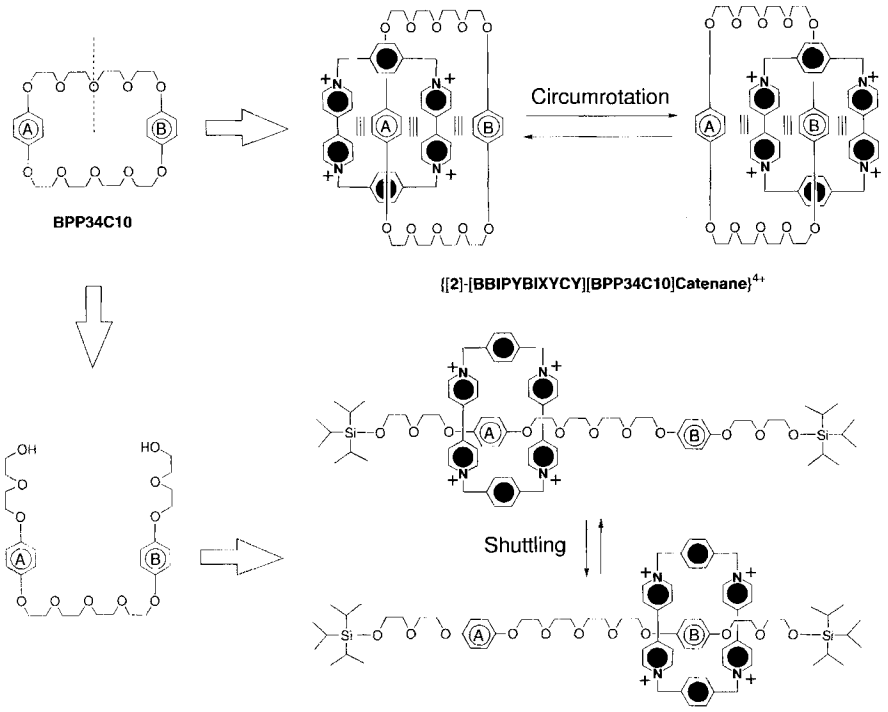

Figure 3. The analogy between the circumrotation of the tetracationic cyclophane component around the crown ether component in a [2]catenane and the possibility of a shuttling process in a [2]rotaxane that directed our attention toward the synthesis of a molecular shuttle.

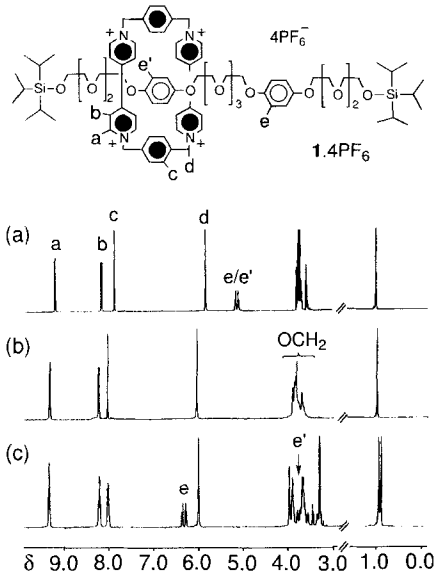

Figure 4. The variable-temperature ^{1}H NMR spectra of the [2]rotaxane **1**·4PF$_6$ recorded a) at 413 K in CD_3SOCD_3; b) at 298 K in CD_3COCD_3; and c) at 223 K in CD_3COCD_3.

exchange of the cyclophane between the two hydroquinone rings is fast, rendering them equivalent on the ^{1}H NMR timescale. ^{13}C NMR spectroscopy was shown in this instance to complement the ^{1}H NMR experiments. In particular, the signals for the hydroquinone ring carbons are not evident in the spectrum recorded in CD_3COCD_3 at room temperature. However, at +75 °C in CD_3CN, shuttling is "fast" and they resonate at $\delta = 153.1$, 152.8 (C), and 115.3 (CH), whereas at −40 °C in CD_3COCD_3 shuttling is "slow" and signals are observed at $\delta = 153.0$, 152.7, and 150.6 (C) and at 115.3, 115.2, 113.4, and 113.3 (CH). The site exchange process in this case is degenerate. Following these encouraging investigations of the shuttling properties of the degenerate [2]rotaxane **1**·4PF$_6$, it was obvious that we should proceed next to reduce the symmetry of the molecular shuttle.

B. The Second Molecular Shuttle: Next, we argued that replacement of one of the two degenerate hydroquinone rings in **1**·4PF$_6$ by a unit of lower π-donating ability should result[16] in a [2]rotaxane in which the preferential population of one translational isomer at low temperature is a possibility. One such suitable candidate[28] for the second station is the *p*-xylyl residue, the oxidation potential of which (+1.8 V) is somewhat higher than that (+1.3 V) of a hydroquinone ring, making it a considerably poorer π-electron donor. Any possibility of exercizing control in such a [2]rotaxane would result from the tetracationic cyclophane preferentially encircling the more π-electron-rich hydroquinone ring. Electrochemical control would then, in principle, be possible by oxidation of the hydroquinone ring to its radical cation, which should, in turn, lead to the preferential encircling of the less π-electron-donating *p*-xylyl ring in the dumbbell-shaped component by the tetracationic cyclophane.

Synthesis: Our synthetic target became the [2]rotaxane **2**·4PF$_6$ (Scheme 3). We envisaged this [2]rotaxane being synthesized by a self-assembly process from the dumbbell-shaped com-

Table 1. Spectroscopic, kinetic, and thermodynamic data [a] associated with processes 1 and 2 in the [2]rotaxanes **1**·4PF$_6$, **3**·4PF$_6$, and **4**·4PF$_6$, as determined by ^{1}H NMR spectroscopy.

[2]Rotaxane	Probe protons		Solvent	$\Delta\nu$ (Hz)	k_c [a] (s^{-1})	T_c (K)	$\Delta G_c^{\ddagger}$ (kcal mol^{-1}) [b,c]	Process
1·4PF$_6$	a	a′	CD_3CN	7.0	16	253	13.3	–
	c	c′	CD_3CN	7.6	17	237	12.4	
	e	e′	CD_3CN	1060	2360	307	13.2	–
3·4PF$_6$	j_1	j_1'	CD_3CN	16	35	253	12.7	1
	i_1	i_1'	CD_3CN	24	53	263	13.0	1
4·4PF$_6$	c_1	c_1'	[D$_7$]DMF	32	71	278	13.9	1
	b_1	b_1'	[D$_7$]DMF	20	44	268	13.6	1
	a_1^x	a_1^y	[D$_7$]DMF	875	1945	373	16.4	2
	c_1	c_1'	CD_3SOCD_3	44	98	338	16.8	1
	b_1	b_1'	CD_3SOCD_3	36	80	333	16.7	1
	c_1	c_1'	CD_3CN	76	169	265	12.7	1
	b_1	b_1'	CD_3CN	52	115	259	12.6	1
	c_1	c_1'	CD_3COCD_3	84	187	274	13.1	1
	b_1	b_1'	CD_3COCD_3	36	80	263	13.0	1

[a] All values of $\Delta G_c^{\ddagger}$ were obtained by the coalescence method. Values for k_c were obtained [I. O. Sutherland, *Ann. Rep. NMR Spectrosc.* **1971**, *4*, 71] from the approximate expression $k_c = \pi - (\Delta\nu)/(2)^{1/2}$. [b] The Eyring equation was used to calculate $\Delta G_c^{\ddagger}$ values at T_c. [c] Several approximations are involved in this semiquantitative treatment, so $\Delta G_c^{\ddagger}$ should be viewed as containing 10% error margins.

0947-6539/97/0307-1116 $ 17.50+.50/0 Chem. Eur. J. 1997, 3, No. 7

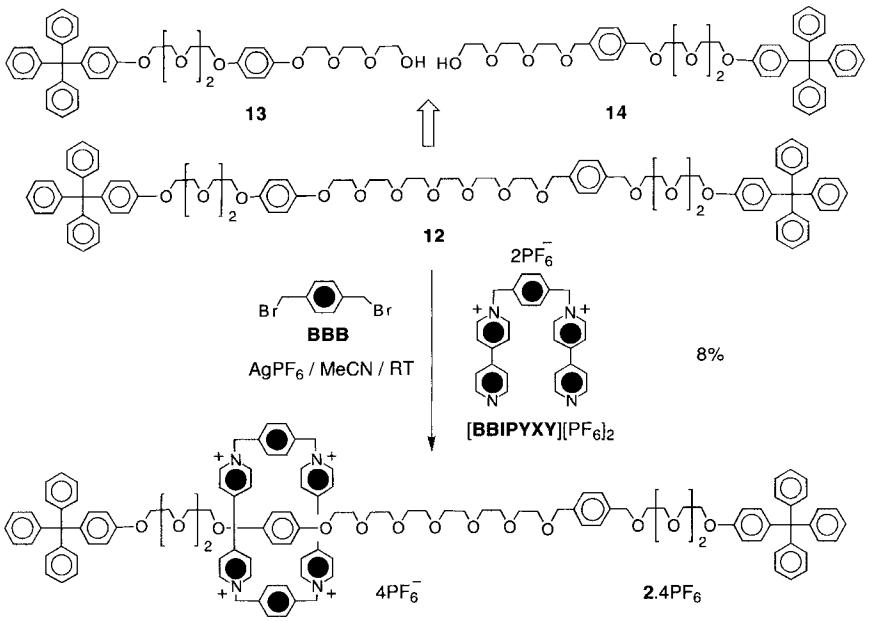

Scheme 3. Synthesis of [2]rotaxane $2\cdot4PF_6$.

pound **12**, $[BBIPYXY]^{2+}$, and BBB. Our approach (Scheme 3) to the synthesis of the asymmetrical compound **12** required the synthesis of two polyether chains within which are located two different recognition sites. Stoppers would then be added to one end of each of the polyether chains. For the stoppers, we chose 4-tritylphenol groups in preference to the triisopropylsilyl ether blocking groups because of the greater stability of tetraarylmethane units under the range of synthetic conditions necessary in the subsequent synthesis. The two polyether precursors **13** and **14**, after appropriate modification, would then be joined together to yield the dumbbell-shaped compound **12**.

The polyether precursor **13** was synthesized in three steps from the known diol **5** (Scheme 4).[111] Monoprotection of the diol (TBDMS/imidazole/DMF) afforded the alcohol **15** (38% yield). Tosylation ($TsCl/Et_3N/CH_2Cl_2$) of **15** (84%), alkylation of the resulting tosylate **16** with 4-tritylphenol (K_2CO_3/DMF), and subsequent deprotection (Bu_4NF/THF) yielded the desired alcohol **13** (44%). The tosylate **17** can be prepared[29] from the diol **18** in four steps (Scheme 4). Monoprotection (41%), tosylation (62%), and alkylation, followed by deprotection, lead to the alcohol **14** (56%). The synthesis of **17** is completed by tosylation ($TsCl/Et_3N/CH_2Cl_2$) of **14** in 62% yield. Compound **12** is then obtained by reaction of the two fragments **13** and **17** under strongly basic conditions (NaH/THF/reflux, Scheme 3).

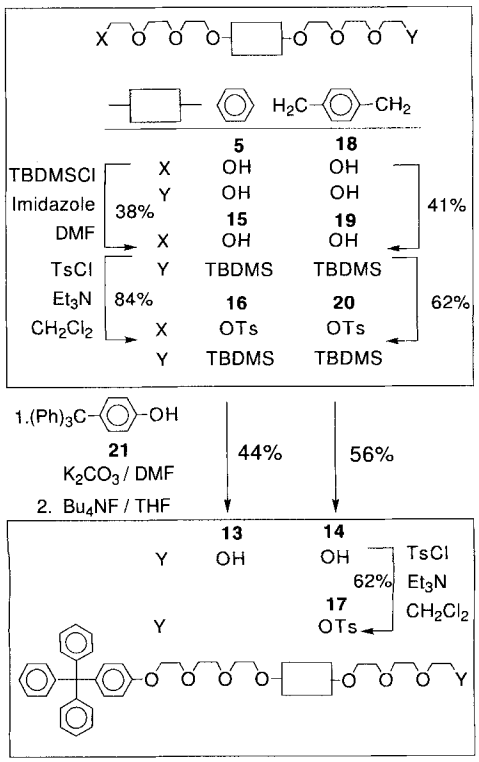

Scheme 4. Synthesis of **13** and **17**.

The self-assembly of the [2]rotaxane $2\cdot4PF_6$ from compound **12** and the components BBB and $[BBIPYXY][PF_6]_2$ can be achieved by stirring them in MeCN under nitrogen for 7 d in the presence of $AgPF_6$ (Scheme 3). After workup and purification by chromatography, the [2]rotaxane $2\cdot4PF_6$ is isolated as orange crystals in 8% yield. The relatively low yield obtained in this particular self-assembly process is probably a reflection of the reduced molecular recognition between the dumbbell-shaped component **12** and the tetracationic cyclophane component formed, possibly as a result of the *p*-xylyl residue contributing very little to the template effect. The low yield, however, is not dissimilar to those reported previously[11, 24] for related template-directed syntheses.

NMR Spectroscopy: The ^1H NMR spectrum of the [2]rotaxane $2\cdot4PF_6$ in CD_3CN varies with temperature and the slow site exchange limit was established below 240 K for selected probe protons. In the discussion that follows, the protons are labeled according to the notation adopted in Figure 5, which depicts the translational isomers 1 and 2. Primes have been used to differentiate nonequivalent sides of the same aromatic rings within the cyclophane. The subscripts 1 and 2 refer to the two translational isomers as depicted in Figure 5. The superscripts h and x refer to protons on the phenolic rings of the terminal tritylphenyl groups of the polyether component depending on whether they are adjacent to the hydroquinone ring or the *p*-xylyl unit, respectively. Since dispersive interactions between the tetracationic cyclophane and the π-electron-rich site account for a sizable fraction of the binding energies involved, we predicted that the cyclophane should encircle preferentially the hydroquinone ring.

The ^1H NMR spectra recorded at 243 and 343 K for the [2]rotaxane $2\cdot4PF_6$ are shown in Figure 6. The protons labelled a–i in Figure 5 were assigned to δ values as a result of a COSY experiment and variable temperature ^1H NMR spectroscopy. These experiments revealed the presence of two different trans-

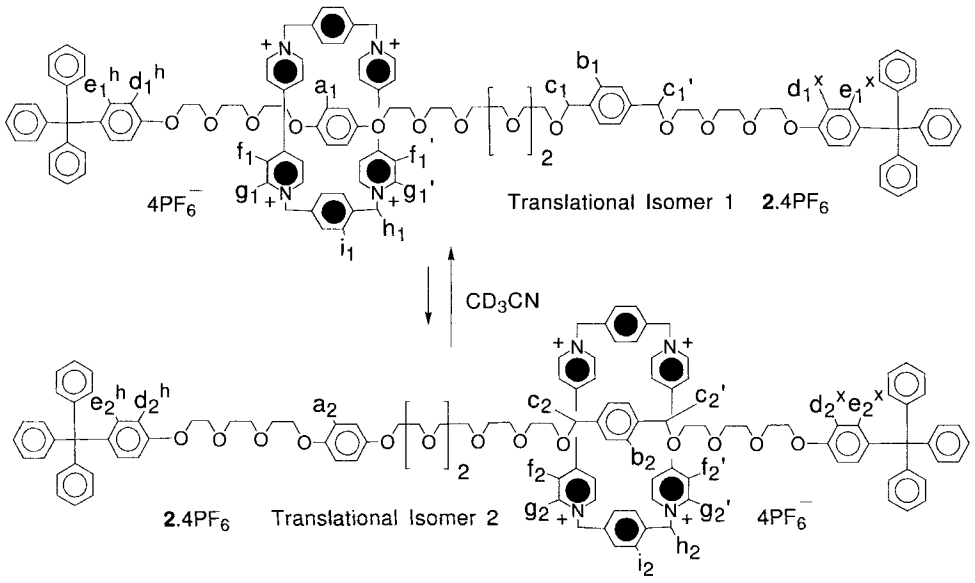

Figure 5. The translational isomers 1 and 2 and the labeling of the protons of the [2]rotaxane **2**·4PF$_6$.

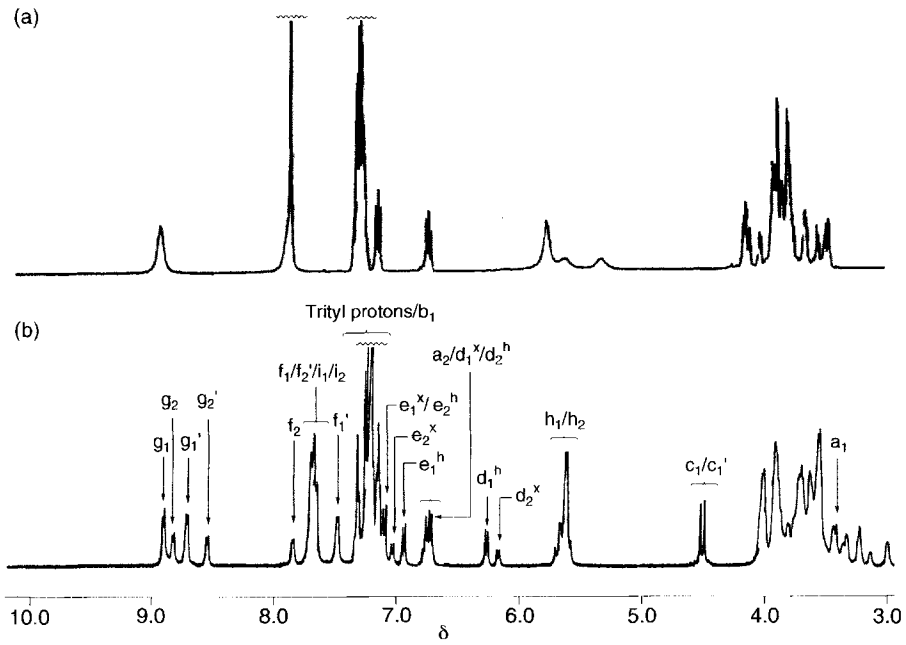

Figure 6. Variable-temperature ^{1}H NMR spectra of the [2]rotaxane **2**·4PF$_6$ recorded in CD_3CN at a) 343 K and b) 243 K.

tons on the three terminal phenyl rings of the tritylphenyl blocking groups were not well resolved and provided no additional information about translational isomerism within **2**·4PF$_6$. The proton signals of the tetracationic cyclophane component provide information about its location on the dumbbell-shaped component. In particular, at 343 K, the α-bipyridinium protons appear as one broad signal, either because of fast shuttling of the cyclophane or rapid spinning of the bipyridinium units within the cyclophane on the ^{1}H NMR timescale (Figure 7). However, at 243 K, the α-bipyridinium signals appear as four separate signals, which consist of two pairs of doublets present in the integrated ratio of 70:30 for the protons $g_1/g_{1'}$ and $g_2/g_{2'}$, respectively. Each translational isomer gives rise to a pair of doublets for the α-bipyridinium protons g since each side of the cyclophane experiences a distinct environment when it is positioned around the unsymmetrically located hydroquinone ring or *p*-xylyl nucleus in the dumbbell-shaped component. Protons g_1 and $g_{1'}$, as well as g_2 and $g_{2'}$, are related by site exchange processes in which the bipyridinium units rotate around their long axes (Figure 7). A similar process has also been observed[30] in the other molecular shuttles discussed in this paper. Analysis of the signals for the β-bipyridinium protons (f) was complicated by coincidence of the signals for the phenylene protons (i_1 and i_2).[31] A COSY experiment established the coupling of the α-bipyridinium protons (g) with the β-bipyridinium protons (f) within this region of the spectrum. The cyclophane methylene protons (h) appear as two signals, h_1 and h_2 at 243 K, the relative integrals of which reflect the distribution of the cyclophane between the hydroquinone ring and *p*-xylyl unit. A COSY experiment identified the hydroquinone protons (a_1 and a_2), since a_1 gives rise to the only isolated signal in the $\delta = 3.0-4.0$ region that is not coupled to another signal and, similarly, a_2 gives rise to the only uncoupled signal in the $\delta = 6.5-7.0$ region. The chemical shift of the signal attributed to a_1 at $\delta = 3.36$ is typical[11] for the protons on a hydroquinone ring that is included within the cavity of the tetracationic cyclophane. The corresponding signal arising from the aromatic protons (b_2) for the *p*-xylyl nucleus should also be present at $\delta = 3.0-4.0$ but this signal could not be identified

lational isomers, which can be inferred from cyclophane proton signals and from signals arising from protons associated with the terminal blocking groups. Since the chemical shifts for the protons d_1^h/e_1^h and d_2^x/e_2^x are different and relate, respectively, to the presence of the cyclophane on either an adjacent hydroquinone ring or on a *p*-xylyl unit, it is possible—from integration of these two pairs of signals—-to deduce that there is 70% of one translational isomer and 30% of the other. Integration of the benzylic methylene signals for the protons c_1 on the unoccupied *p*-xylyl nucleus (not *J*-coupled with any other signal, according to the COSY spectrum) indicates that translational isomer 1, in which the tetracationic cyclophane occupies a position around the hydroquinone ring, is the major species present at equilibrium at 243 K. The signals pertaining to pro-

0947-6539/97/0307-1118 $ 17.50+.50/0 Chem. Eur. J. 1997, 3, No. 7

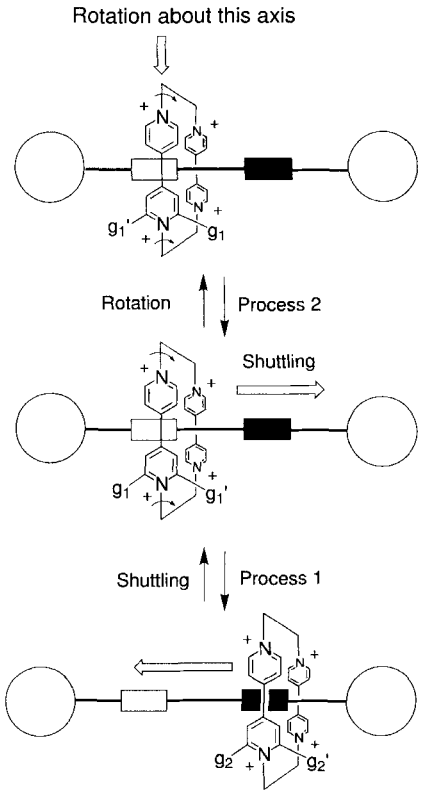

Figure 7. Diagram showing exchange processes 1 and 2 (shuttling and rotation processes, respectively) that constitute the site exchange processes detectable by ^{1}H NMR spectroscopy. The α-bipyridinium protons are labeled.

from amongst the signals associated with the OCH_2 protons. The signal for the aromatic protons b_1 was assumed to lie underneath the multiplet arising from protons in the trityl groups.

The dynamic properties of this molecular shuttle were investigated by variable-temperature ^{1}H NMR spectroscopy. The fast exchange limit for all the protons was reached at 343 K (Figure 6). Two dynamic processes (Figure 7) can operate within this [2]rotaxane: 1) shuttling of the cyclophane between the hydroquinone ring and the *p*-xylyl unit (process 1 in Figure 7), and 2) rotation of the bipyridinium units of the cyclophane about their long axes leading to exchange of the primed and unprimed protons (the rotation process 2 shown in Figure 7). Both of these site exchange processes could be operating simultaneously in the coalesence of the two pairs of doublets associated with the α-bipyridinium protons (g) to one broad doublet observed at 343 K for **2**·4PF_6. Consequently, it was not possible to ascertain the energy barrier associated with processes 1 and 2 by consideration of the variable temperature ^{1}H NMR spectra of the α-bipyridinium signals (g).[32]

Reflections and an Improved Strategy: So far, we have demonstrated that the location within the dumbbell-shaped component of a new π-electron donor, the affinity of which for the tetracationic cyclophane is less than that of a hydroquinone ring, leads to the predominance of one translational isomer over the other. This predominance is in favor of the recognition site with the lower oxidation potential, that is, in the case of **2**·4PF_6, the more π-electron-donating hydroquinone ring. The problems in pursuing this strategy are twofold: the use of a less effective recognition unit than the hydroquinone ring suggests that, in order to improve upon the relative translational isomer ratio of 70:30, we run the risk of lowering the overall yield obtained in a template-directed synthesis; furthermore, the sensitivity of the hydroquinone radical cation detracts from its use as an electrochemically addressable species. An improved strategy for the construction of an electrochemically addressable molecular shuttle is outlined in Figure 8. Site A (the non-hydroquinone

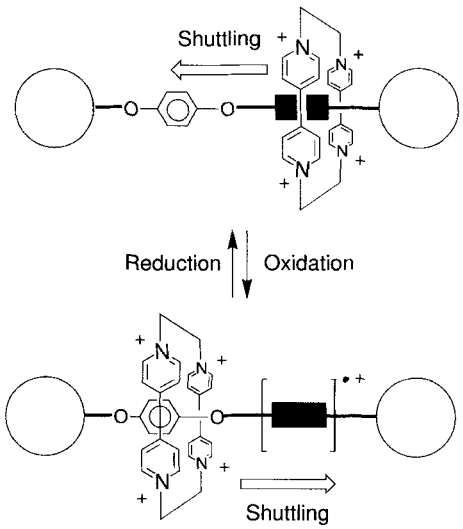

Figure 8. A schematic representation of a strategy in which a better π-electron donor (site A) than a hydroquinone ring will be occupied preferentially by the tetracationic cyclophane until it is oxidized. The cyclophane, which is subjected to a charge–charge repulsion as well as to the loss of any stabilizing donor–acceptor interactions, prefers to shuttle to the hydroquinone ring site until such time as site A is reduced back to its neutral state.

site) should satisfy two criteria: it should have a larger binding constant with the tetracationic cyclophane than the hydroquinone ring (HQ) and it should have a lower oxidation potential than HQ. The benefits of altering the design logic in this manner include 1) a potentially higher yield during the self-assembly of the [2]rotaxane as a result of enhanced templating interactions and 2) the incorporation of more electrochemically robust units into the dumbbell-shaped component. Oxidation of site A should cause the cyclophane to move to the hydroquinone ring. In summary, the π-electron donor chosen for site A must fulfil the following criteria: 1) be easily oxidizable; 2) form a stable radical cation; 3) have a small steric size that permits it to enter inside the rigid tetracationic cyclophane; and 4) have an oxidation potential different from that of the hydroquinone ring (at least 0.3 V less positive). The remainder of this discussion relates the progress we have made in realizing such an electrochemically controllable molecular shuttle.

C. The Third Molecular Shuttle: A 2,3,5-trisubstituted indole residue was identified[34] as satisfying most of the criteria listed at the end of Section B. Since the tetracationic cyclophane is known to form a strong complex with tryptophan,[35] we decided to investigate the incorporation of an indole unit into an asymmetric [2]rotaxane.[17] Initially, we examined the complexation of the model indole by cyclobis(paraquat-*p*-phenylene) (Scheme 5). When a molar equivalent of **24** is added to a solu-

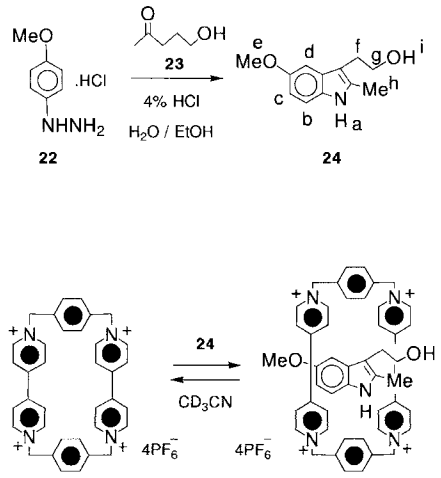

Scheme 5. Complexation of the model indole by cyclobis(paraquat-*p*-phenylene).

tion of the tetracationic cyclophane in CD_3CN, a deep purple color results. ^1H NMR spectroscopic data suggests that the indole ring is threaded through the macrocycle in a rotaxane-like manner (Table 2).

Table 2. ^1H NMR spectroscopic evidence for complex formation between the indole derivative **24** and cyclobis(paraquat-*p*-phenylene) tetrakis(hexafluorophosphate) in CD_3CN.

Proton	δ Free	δ Complex	$\Delta\delta$
a	8.77	8.22	−0.55
b	7.13	6.33	−0.80
c	6.65	6.33	−0.32
d	6.94	5.99	−0.95
e	3.77	3.67	−0.10
f	2.82	2.70	−0.12
g	3.62	3.58	−0.04
h	2.58	2.81	+0.23
i	2.31	2.30	−0.01

X-Ray Crystallography of 1:1 Complex formed between Cyclobis(paraquat-p-phenylene) and 2-Methylindole: Crystals suitable for X-ray analysis were grown by vapor diffusion of iPr_2O into an MeCN solution containing an equimolar mixture of [BBIPYBIXYCY][PF_6]$_4$ and 2-methylindole (2 MIN). An interesting feature about the 1:1 complex is its distinctive purple color. The solid-state structure of [BBIPYBIXYCY·2 MIN][PF_6]$_4$ shows the 2 MIN molecule to be inserted through the center of the tetracationic cyclophane with its long axis steeply inclined (66°) to the mean plane of the cyclophane (Figure 9a). There is a crystallographically imposed symmetry center upon the 1:1 complex, requiring the 2 MIN molecule to be disordered. In addition to this C_i disorder, it is not possible to rule out secondary C_2 rotational disorder of the 2 MIN molecule about its long axis (this was allowed for in the structure refinement process). The overall dimensions of the tetracationic cyclophane are unchanged from those observed for the related TTF complex, vide infra. The twist and bow angles for the bipyridinium units are 8° and 23°, respectively. The disorder of the included indole molecule prevents a detailed analysis of any [C–H···π] or [N–H···π] interactions to the *p*-xylyl rings,

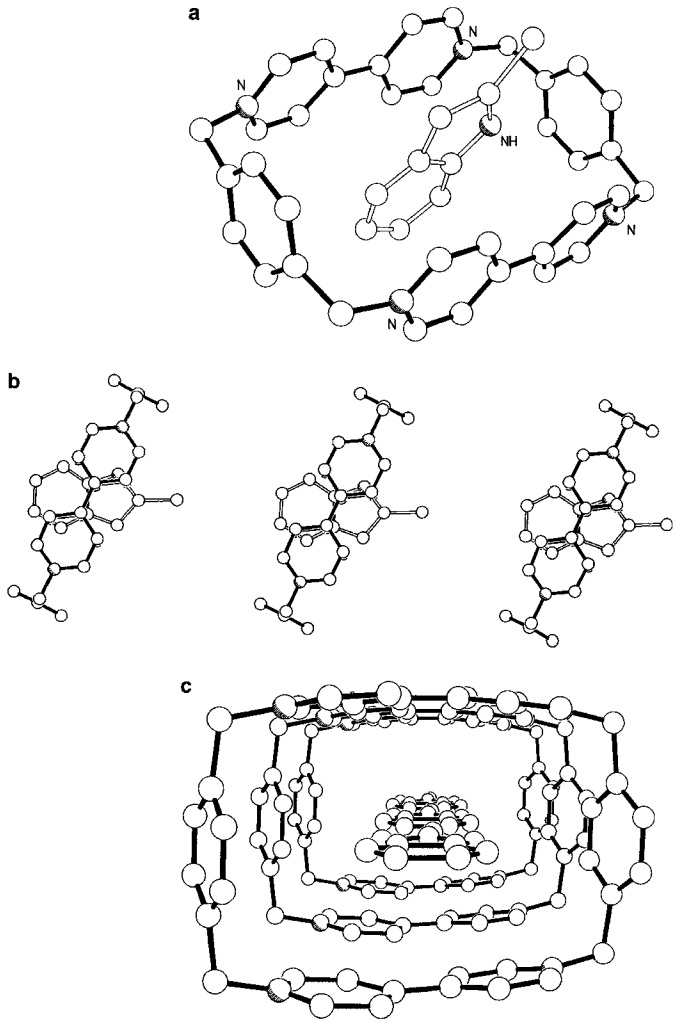

Figure 9. a) Ball-and-stick representation of the solid-state structure of [BBIPYBIXYCY·2 MIN]$^{4+}$. b) Side-on and c) end-on views of the stepped stack-like superstructure of the 1:1 complex in one of the crystallographic directions.

though these are almost certainly present at ca. 2.7 Å ([H···π]) as a consequence of the tilt of this unit within the cyclophane. Although the geometry of this 1:1 complex is very similar to that of the TTF analogue, the supramolecular structure is different. The TTF complex crystallizes in the triclinic space group $P\bar{1}$, whereas the 2 MIN complex has monoclinic crystal symmetry with space group $P2_1/n$ and is, at the crystallographic level, isomorphous with a range of simple complexes involving the tetracationic cyclophane.[20] In this latter structural arrangement, the tetracationic cyclophanes are stacked in the crystallographic *a* direction and have the encapsulated 2 MIN molecules co-aligned (Figures 9b and c). The approximate distance between the methyl group on the five-membered ring and the center of the nearest facing indole C–C bond within the stack is 4.7 Å compared with 4.9 Å in the TTF analogue. The *p*-xylyl units of adjacent stacks are in a stepped and sheared arrangement with an interplanar separation of 3.2 Å and a centroid–centroid separation of 4.9 Å. Pairs of methylene hydrogen atoms in one stack are directed into the π-system of the *p*-xylyl ring of an adjacent stack and vice versa ([H···π] distance, 3.0 Å). There is no stacking relationship between the bipyridinium units.

0947-6539/97/0307-1120 $ 17.50+.50/0 Chem. Eur. J. 1997, 3, No. 7

Synthetic Strategy: We argued that the tetracationic cyclophane should preferentially occupy the indole unit within the dumbbell-shaped component of a [2]rotaxane comprising an indole unit and hydroquinone ring. Oxidation of the indole unit to its radical cation should result in the transfer of the tetracationic cyclophane to the hydroquinone ring. Thus, our synthetic target was identified as the [2]rotaxane $3\cdot 4PF_6$ containing one indole unit and one hydroquinone ring incorporated within a polyether chain terminated by tetraphenylmethane stoppers (Scheme 6). We envisaged that this [2]rotaxane might be self-assembled from the dumbbell-shaped compound **25**, BBB, and [BBIPYXY]-$[PF_6]_2$ using template direction. It was anticipated that **25** would be constructed by a Fischer-indole procedure[36] from the Boc-protected hydrazine **26** and the ketal **27** in which the two protecting groups are removed in situ prior to the two fragments combining to form the indole system in one step.

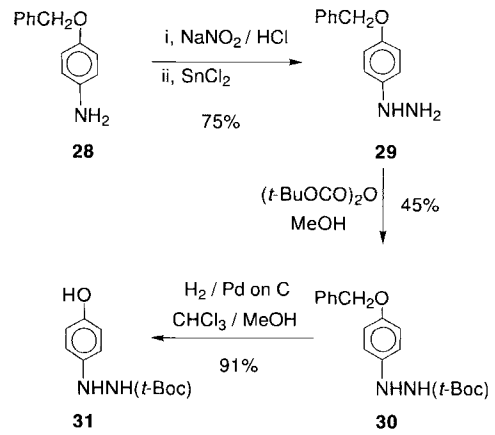

Scheme 7. Preparation of **31**.

Synthesis: The synthesis of the fragment **26** was achieved in four steps from the commercially available 4-benzyloxyaniline **28** (Schemes 7 and 8). Diazotization ($NaNO_2$/HCl) of **28** followed by reduction ($SnCl_2$) gave the corresponding hydrazine **29** as the hydrochloride salt in 75% yield overall. Protection ($(tBoc)_2O$/MeOH, 45%) of the hydrazine, followed by removal (H_2/Pd/C/MeOH/$CHCl_3$ 1:1, 91%), of the benzyl ether protecting group from **30** gave the phenol **31**. Reaction (K_2CO_3/DMF) of this phenol with the tosylate **33** (derived from 4-tritylphenol following its base-promoted (K_2CO_3/MeCN) reaction with chloroethoxyethanol **9** to give **32**, which was subsequently tosylated (TsCl/ NEt_3/CH_2Cl_2)) gave **26** in 46% yield. The ketal **27** was obtained in a single step (51% yield) by the reaction of **13** and 5-chloro-2-pentanone ethylene ketal **34** under strongly basic conditions (NaH/THF, Scheme 9). The synthesis of **25** was completed in 51% yield by coupling the ketal **27** and hydrazine derivative **26** under mild conditions (1% HCl/aq. EtOH; Scheme 6).

The [2]rotaxane $3\cdot 4PF_6$ was self-assembled (Scheme 6) from the dumbbell-shaped compound **25**, BBB, and [BBIPYXY]-$[PF_6]_2$ in MeCN solution under template-directing conditions in 9% yield. FABMS of $3\cdot 4PF_6$ showed the presence of a peak at $m/z = 2271$ consistent with the loss of one hexafluorophosphate counterion from the [2]rotaxane.

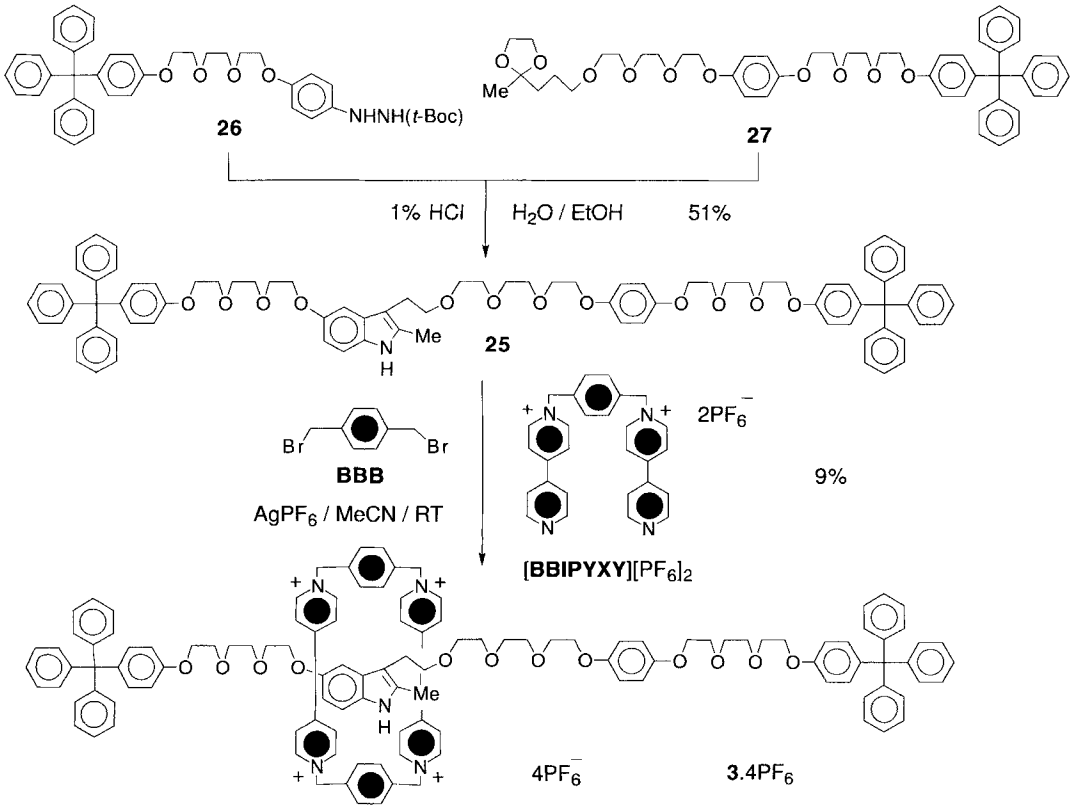

Scheme 6. Synthesis of the [2]rotaxane $3\cdot 4PF_6$ containing one indole unit and one hydroquinone ring incorporated within a polyether chain terminated by tetraphenylmethane stoppers.

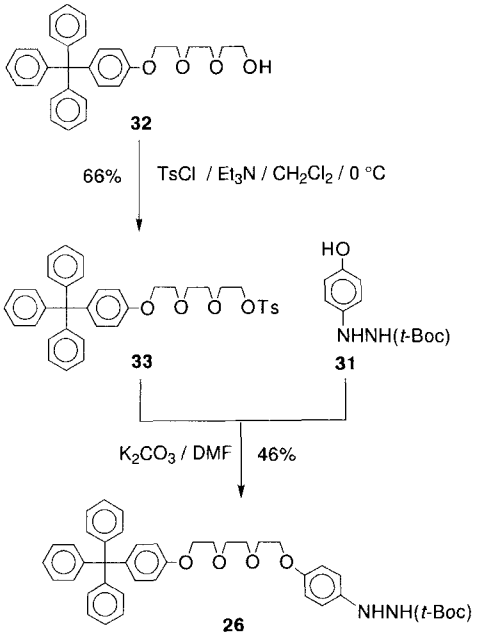

Scheme 8. Synthesis of the fragment **26**.

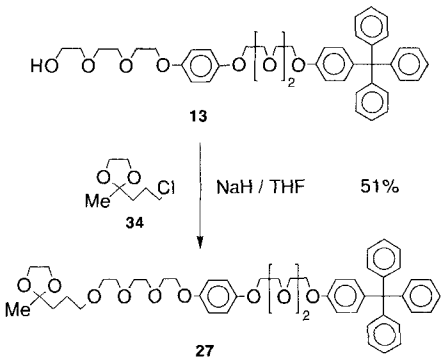

Scheme 9. Synthesis of ketal **27**.

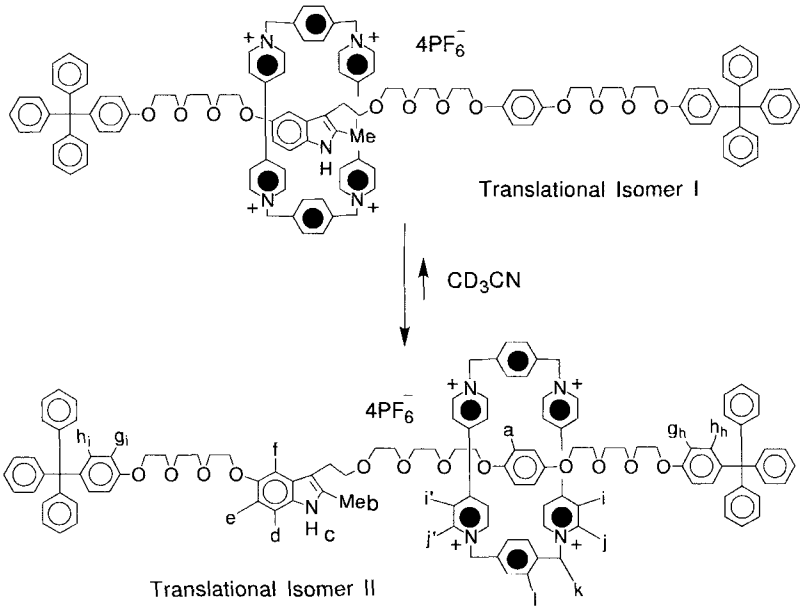

Figure 10. The translational isomers 1 and 2 and the labeling of the protons in the [2]rotaxane $3\cdot4PF_6$.

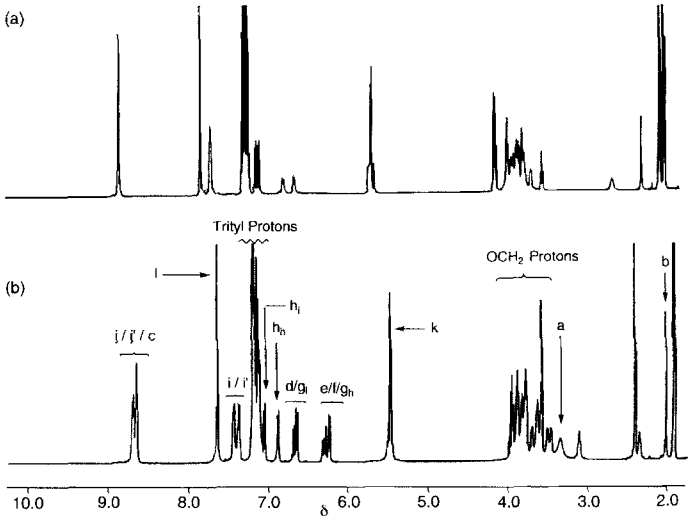

Figure 11. Variable-temperature ^{1}H NMR spectra of the [2]rotaxane $3\cdot4PF_6$ recorded in CD_3CN at a) 343 K and b) 233 K.

^{1}H NMR Spectroscopy: The assignment of the proton resonances in $3\cdot4PF_6$ was made in CD_3CN. The ^{1}H NMR spectrum recorded in this solvent varies with temperature and the slow site exchange limit was established below 230 K for all protons. In the discussion that follows, the protons are labeled according to the notation in Figure 10. Primes have been used to differentiate constitutionally identical protons on opposite sides of the tetracationic cyclophane. The subscripts i and h refer to protons on the phenolic rings of the terminal tritylphenyl groups of the dumbbell-shaped component, depending on whether they are adjacent to the indole nucleus or hydroquinone ring, respectively.

The complete ^{1}H NMR spectrum recorded at 233 K for $3\cdot4PF_6$ is shown in Figure 11. The protons labeled a–l in Figure 10 were assigned by a COSY experiment, which revealed the presence of only one translational isomer at low temperature. Examination of the COSY spectrum indicates an uncoupled signal resonating at $\delta = 3.38$ (labeled a in Figure 10), which is characteristic of a hydroquinone ring included within the cavity of the tetracationic cyclophane. This observation, in combination with the essentially unchanged chemical shifts—compared with those in the dumbbell-shaped compound **25**—for signals arising from the protons on the indole nucleus, indicates that the tetracationic cyclophane encircles the hydroquinone ring almost exclusively at low temperature. The protons on the phenolic rings of the tritylphenyl blocking groups appear as only two AB-like systems, again reflecting the close to exclusive occupation of only one of the two possible donor sites within the dumbbell-shaped component of $3\cdot4PF_6$. The signals for the other aromatic protons on the tritylphenyl blocking groups were not so well resolved and provided no additional information about the positioning of the cyclophane component within the [2]rotaxane.

The location of the cyclophane component in $3\cdot4PF_6$ is also indicated by the signals for the α- and β-bipyridinium protons (j and i, respectively) on the tetracationic cyclophane (Figure 11). At 343 K, protons j and i resonate as single doublets at $\delta = 9.11$ and 7.47, respectively, on account of rapid rotation of the

0947-6539/97/0307-1122 $ 17.50+.50/0 Chem. Eur. J. 1997, 3, No. 7

bipyridinium units within the cyclophane component on the ^{1}H NMR timescale (Process 2, Figure 7). At the slow exchange limit at 233 K, two separate doublets of equal intensity are observed for both bipyridinium protons as a consequence of the nonequivalence of the two edges of the cyclophane when it encircles the unsymmetrically located hydroquinone ring within the dumbbell-shaped component. The methylene protons (k) and phenylene protons (l) in the cyclophane both appear as one signal at 243 K; this again reflects the fact that only one translational isomer is populated in **3**·4PF$_6$ at this temperature. The calculated free energy barriers for process 2 are listed in Table 1. The average $\Delta G^{\ddagger}$ value of 12.9 kcal mol^{-1} is identical with that observed for the same process in the TTF shuttle **4**·4PF$_6$ in CD_3CN. It should be stressed that the temperature dependence of the ^{1}H NMR spectrum of **3**·4PF$_6$ can only be interpreted in terms of the operation of process 2 since only one translational isomer is populated at low temperature.[37]

Reflections and Conclusion: Thus, although the indole unit is the more π-electron-rich site, it is also the more sterically demanding and so the hydroquinone ring is included preferentially within the cyclophane. The low yield observed in the self-assembly of **3**·4PF$_6$ most probably reflects not only the nonideal nature of the central polyether chain but also the steric hindrance encountered by the developing tetracationic cyclophane. Obviously, the decisive preference for this rotaxane to yield the "unwanted" translational isomer meant that this system was not suited to electrochemical control.

D. The Fourth Molecular Shuttle: An initial study of the binding of a range of different substrates with the tetracationic cyclophane receptor allowed us to identify other potential binding sites in [2]rotaxanes from a broad range of π-electron-rich substrates. One such substrate, which was found to have a high affinity for the tetracationic cyclophane[20] and which also displays highly reversible redox behavior at low potentials,[38] is tetrathiafulvalene (TTF). Mixing equimolar mixtures of [BBIPYBIXYCY][PF$_6$]$_4$ and TTF in MeCN produces an emerald-green solution as a result of the charge-transfer interactions between the π-electron-rich TTF unit and the π-electron-deficient tetracationic cyclophane. Two methods were used to calculate the value of K_a for the equilibrium shown in Scheme 10.[39] A spectrophotometric titration[40] performed at 854 nm in MeCN yielded a value for K_a of $8030 \pm 535\,M^{-1}$ for the 1:1 complex (Scheme 10) formed between [BBIPYBIXYCY][PF$_6$]$_4$ and TTF, while a dilution method[41] based on ^{1}H NMR chemical shift data gave a value for K_a of $7190 \pm 970\,M^{-1}$ for the same equilibrium in MeCN.

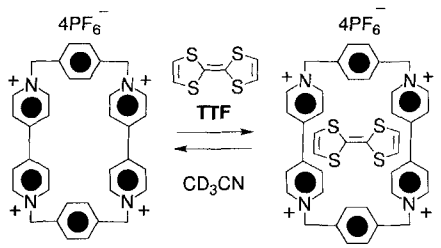

[BBIPYBIXYCY][PF$_6$]$_4$ **[TTF.BBIPYBIXYCY][PF$_6$]$_4$**

Scheme 10. Equilibrium between [BBIPYBIXYCY][PF$_6$]$_4$ and TTF in MeCN.

X-Ray Crystallography of a 1:1 Complex formed between Cyclobis(paraquat-p-phenylene) and Tetrathiafulvalene: Crystals suitable for X-ray structural analysis were grown by vapor diffusion of iPr_2O into solutions containing an equimolar mixture of [BBIPYBIXYCY][PF$_6$]$_4$ and TTF in MeCN. The [BBIPYBIXYCY·TTF][PF$_6$]$_4$ complex is green both in solution and in the solid state. The X-ray structural analysis of [BBIPYBIXYCY·TTF][PF$_6$]$_4$ reveals the TTF molecule to be inserted centrosymmetrically through the tetracationic cyclophane with its long axis steeply inclined (66°) to the mean plane of the cyclophane, which has overall dimensions of 6.9 and 10.3 Å (Figure 12a,b). There are characteristic twisting and bowing distortions within the tetracationic cyclophane, that is, 9° twists between the pyridinium rings and a 25° inclination of the two N–CH_2 bonds. Within the 1:1 complex, the distance from each of a diametrically opposite pair of TTF sulfur atoms and their proximal *p*-xylyl ring centroids is 3.31 Å. The 1:1 complexes pack to form stacks (Figure 12c) that extend in all

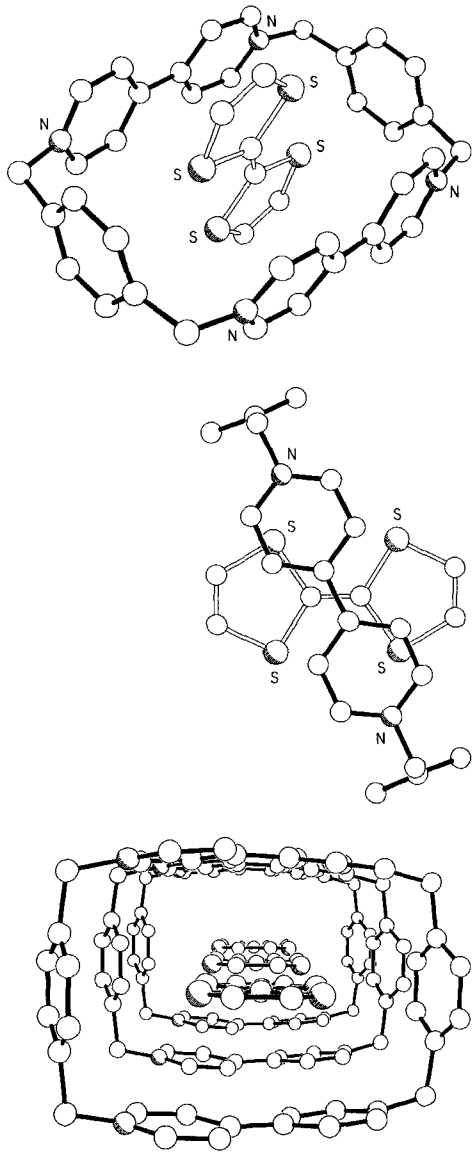

Figure 12. a) Ball-and-stick representation of the solid-state structure of [BBIPYBIXYCY·TTF]$^{4+}$. b) Side-on and c) end-on views of the stepped stack-like superstructure of the 1:1 complex in one of the crystallographic directions.

three crystallographic directions. In the *a* direction, continuous channels are present within the long axes of the TTF molecules and are co-aligned, the shortest inter-TTF [$CH_2 \cdots CH_2$] distance being 4.9 Å. In the *b* direction, the bipyridinium units within adjacent tetracations are arranged to form a stepped stack with a mean interplanar separation of 3.2 Å and a centroid–centroid separation of 5.5 Å. In the *c* direction, a similar stepped stacked arrangement is formed between adjacent *p*-xylyl units in neighboring complexes. The interplanar separation between the *p*-xylyl units is 3.2 Å and their centroid-centroid separation is 5.1 Å. Accompanying this latter sheared arrangement, one of the methylene hydrogen atoms of one cyclophane is directed toward the *p*-xylyl face of another and vice versa. The [$H \cdots \pi$] distance, however, is somewhat long at 3.0 Å and can only represent a very weak but cooperative pair of [$C-H \cdots \pi$] interactions.[42]

Synthetic Strategy: The rotaxane-like orientation of TTF when it is included within the cavity of the tetracationic cyclophane (Figures 12a,b) makes the introduction of a TTF unit into the dumbbell-shaped component of a [2]rotaxane attractive. We selected a bis(2-oxypropylenedithio)TTF derivative for this purpose;[43] the hydroquinone ring was chosen as the less π-electron-rich unit. An efficient synthesis of a dumbbell-shaped compound containing the TTF and hydroquinone unit was from fragment **35**, which self-couples in the presence of triethyl phosphite to yield the dumbbell-shaped compound **36**, in which a hydroquinone ring is located on each side of the TTF nucleus. The outlined approach (Scheme 11) is convenient in that it involves the coupling of identical fragments and, in addition, may favor occupation of the central TTF unit by the tetracationic cyclophane in the [2]rotaxane **4**·4PF_6 since the optimum π-stacking interactions are possible between π-donors and π-acceptors in this translational isomer. We envisaged self-assembling the [2]rotaxane **4**·4PF_6 using template direction in a similar procedure to that already employed for the synthesis of the [2]rotaxanes **1**–**3**·4PF_6.

Synthesis: The fragment **35** may be prepared (Schemes 12 and 13) in eight steps starting from the mixture of diastereoisomers of the 1,3-benzylidene acetal **37**.[44] 2-Phenyl-5-hydroxy-1,3-dioxane **37** was alkylated (Scheme 12) with *t*-butylbromoacetate

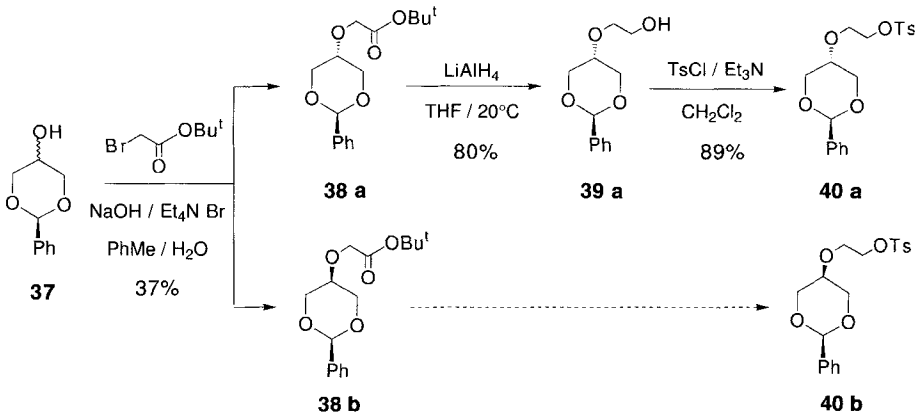

Scheme 12. Synthesis of **40a,b**.

under phase transfer conditions ($NaOH/Et_4NBr/PhMe/H_2O$) to yield (37%) two diastereoisomeric esters of 2-phenyl-5-[2-(*tert*-butoxy)-2-oxoethoxy]-1,3-dioxane (**38a,b**), which could be separated by column chromatography (SiO_2: EtOAc/light petroleum, 1:4). Although both diastereoisomers **38a** and **38b** are equally suitable for use in subsequent syntheses, we chose to proceed only with the *trans*-isomer **38a**, reducing it to the corresponding alcohol **39a** ($LiAlH_4$/THF, 80%), which was then converted ($TsCl/Et_3N/CH_2Cl_2$) to its tosylate **40a** in 89% yield. This tosylate becomes the link between the alcohol **13** and the 2-oxypropylene-4,5-dithio-2-one-1,3-dithione unit. Reaction (NaH/THF) of **40a** with **13** afforded the intermediate **41** in 97% yield (Scheme 13). The benzylidene protecting group was then removed ($H_2SO_4/EtOH/H_2O$, 71%) from **41**, giving the corresponding diol **42**, which was converted ($TsCl/Et_3N/CH_2Cl_2$, 94%) into its ditosylate **43**. Reaction of **43** with the dithiolate dianion, derived from the saponification (NaOMe/MeOH/PhH) of

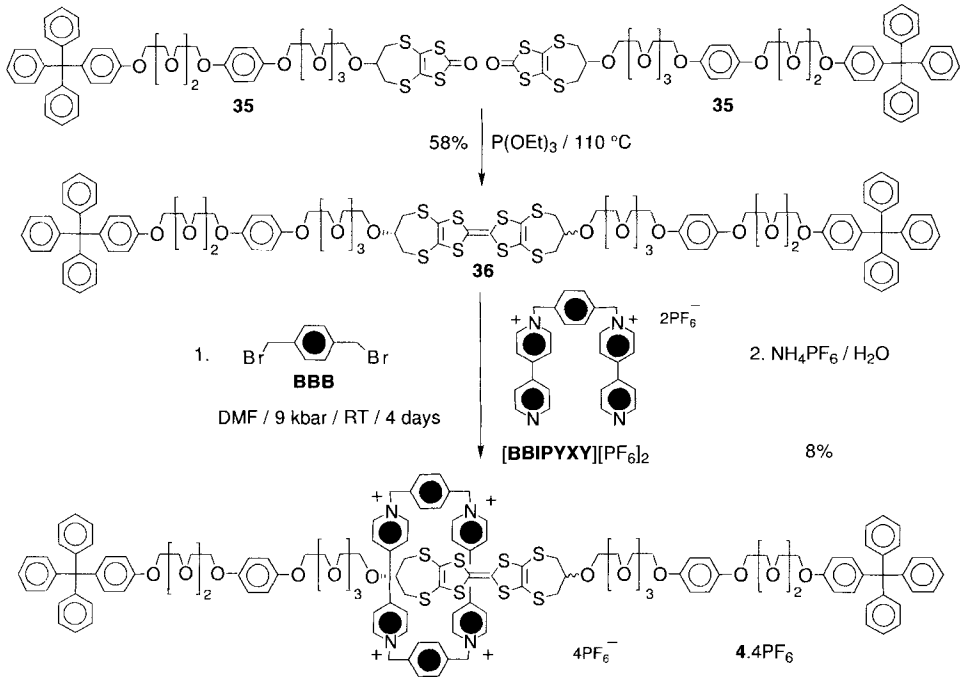

Scheme 11. Synthesis of [2]rotaxane **4**·4PF_6.

0947-6539/97/0307-1124 $ 17.50+.50/0 Chem. Eur. J. 1997, 3, No. 7

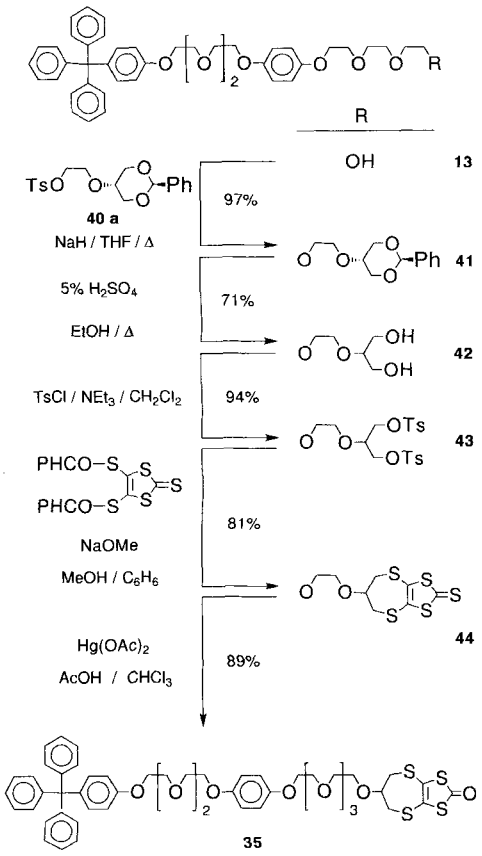

Scheme 13. Synthesis of **35**.

dibenzoyl-4,5-dithio-1,3-dithiol-2-thione[45] afforded the 2-oxypropylene-4,5-dithio-1,3-dithiol-2-thione derivative **44** in 81% yield. Conversion ($Hg(OAc)_2$/AcOH/$CHCl_3$) of **44** into its keto analogue provided the desired fragment **35**. Coupling of **35** (Scheme 11) in neat triethyl phosphite at 110 °C afforded the required TTF-containing dumbbell-shaped compound **36** as an orange oil in 58% yield. ^{1}H NMR spectroscopy reveals that this product exists as a mixture of two diastereoisomers, which we were unable to separate by column chromatography.

The corresponding [2]rotaxane **4**·4PF_6 was self-assembled (Scheme 11) by subjecting the dumbbell-shaped compound **36**, BBB, and [BBIPYXY][PF_6]$_2$ to a pressure of 9 kbar in DMF at room temperature for 96 h. After workup and counterion exchange, the [2]rotaxane **4**·4PF_6 was isolated as small orange crystals in 8% yield.[46]

NMR Spectroscopy: The ^{1}H NMR spectrum of **4**·4PF_6 is both solvent- and temperature-dependent. Examination of spectra in different solvents reveals that a number of exchange processes are occurring on the ^{1}H NMR timescale. In CD_3CN, [D_7]DMF, CD_3NO_2, and CD_3COCD_3, all the resonances are broad at ambient temperature as a consequence of these exchange processes. At ambient temperature in CD_3SOCD_3, however, a well-resolved spectrum is observed as a result of slow exchange. Presumably, the activation energies of the various exchange processes are larger in CD_3SOCD_3, compared with those observed in the other solvents investigated as a consequence of the much higher viscosity of CD_3SOCD_3. A detailed discussion of the ^{1}H NMR spectroscopic behavior of **4**·4PF_6 will be confined to studies carried out in [D_7]DMF, since the wide temperature range (223–410 K) afforded by this solvent enabled a complete analysis of all the different exchange processes. In the discussion that follows, the aromatic protons have been labeled with letters according to the notation described in Figure 13. Primes have been used to differentiate nonequivalent sides of the same aromatic rings within the cyclophane. The numerical subscripts 1 and 2 refer to the two translational isomers as depicted in Figure 13. The superscripts x and y refer to hydroquinone ring protons within translational isomer 1 that are and are not encircled by the tetracationic cyclophane, respectively. The signals for the SCH_2, OCH and OCH_2 groups were broad and complicated and so provided little information about the behavior of the tetracationic cyclophane within the [2]rotaxane.

The full ^{1}H NMR spectra of **4**·4PF_6 in [D_7]DMF recorded at 223, 298, and 338 K are shown in Figure 14. The signals associated with protons a–e were assigned by means of a COSY experiment, which revealed that the tetracationic cyclophane exists in two different environments. For example, the methylene protons (e) of the cyclophane resonate (Figure 14) as two singlets of unequal intensity at $\delta = 6.02$ and 6.17. Integration of these two signals affords the relative populations of the major and minor translational isomers. Examination of the signals for the bipyridinium protons provides a means of determining which of the two translational isomers 1 or 2 predominates. The α- and β-bipyridinium protons, labeled b and c, both resonate as three signals at 223 K. In each case, two of these three

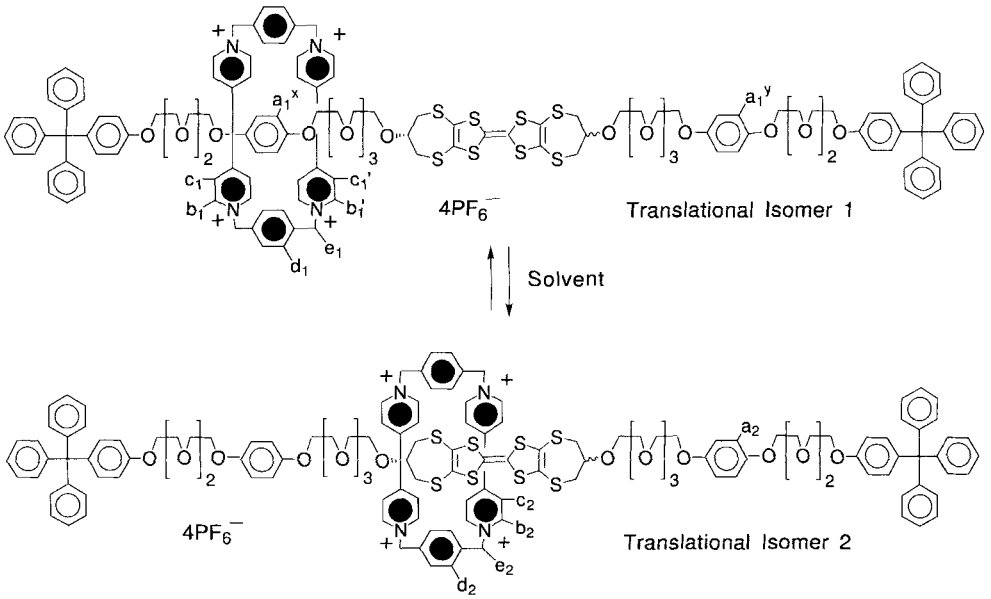

Figure 13. The translational isomers 1 and 2 and the labeling of the protons of the [2]rotaxane **4**·4PF_6.

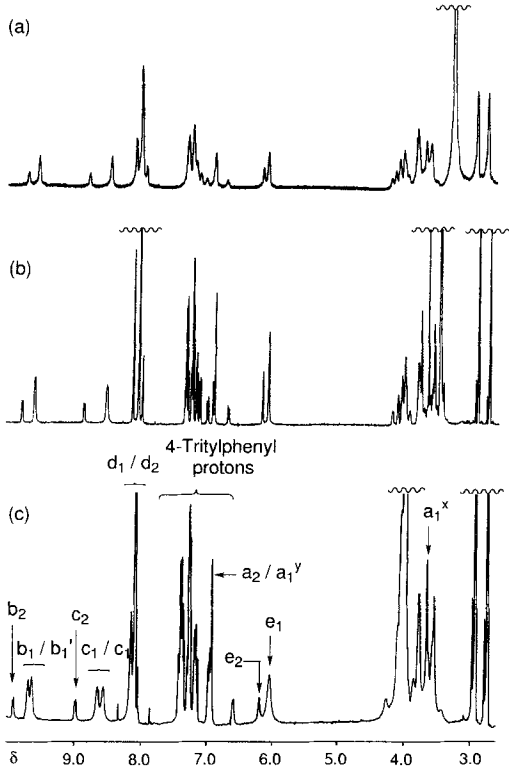

Figure 14. Variable-temperature ^{1}H NMR spectra of the [2]rotaxane **4**·4PF$_6$ recorded in [D$_7$]DMF at a) 223 K, b) 298 K, and c) 338 K.

signals are of equal intensity and one is of lesser intensity. The larger pair of signals corresponds to translational isomer 1 and arises as a result of the nonequivalence of the two edges of the cyclophane in this translational isomer. Rotation of the bipyridinium units around their long (N···N) axes allows the pair of bipyridinium protons in both the a and b positions to exchange environments. A COSY spectrum at 223 K established an AB-like coupling pattern for the α- and β-bipyridinium proton signals in the two translational isomers. By warming the sample, it is possible (Figure 14) to observe coalescence of signals b_1 and $b_{1'}$ and of signals c_1 and $c_{1'}$. The activation energy for this site exchange process is considerably less than that for the shuttling of the cyclophane between hydroquinone ring sites as discussed subsequently. Consequently, the lower energy exchange process was assigned to rotation of the bipyridinium units around their long (N···N) axes, which can only be observed in or around the energy minimum associated with translational isomer 1. Integration of the signals for protons b and c indicates (Figure 14) that the ratio of translational isomers 1:2 is 71:29 in [D$_7$]DMF at 300 K.

The temperature-dependent behavior of the proton resonances a–e also provides useful information about the kinetics of the shuttling process. At 223 K, the hydroquinone ring protons a_1^y and a_1^x resonate as two singlets at $\delta = 6.89$ and 3.65, respectively. A NOESY spectrum shows that these protons are related by a site exchange process. In translational isomer 2, the hydroquinone ring protons a_2 resonate at $\delta = 6.89$. The chemical shifts of the protons a–e of **4**·4PF$_6$ in a variety of deuterated solvents at the slow exchange limit are listed in Table 3. In the other deuterated solvents investigated, the slow exchange limit was observed at the following temperatures: at 243 K in CD$_3$CN, at 233 K in CD$_3$COCD$_3$, and at 300 K in CD$_3$SOCD$_3$. In CD$_3$NO$_2$, the slow exchange limit could not be attained before the freezing point (ca. 248 K) of the solvent was reached. The ^{1}H NMR spectra obtained in these solvents at the indicated temperatures were similar to that recorded in [D$_7$]DMF at 223 K, except for some changes introduced by the different relative populations of translational isomers 1 and 2 as determined by integration of the signals for the bipyridinium protons b and c. The relative populations of these isomers in the range of solvents at room temperature are listed in Table 4.

Table 3. Chemical shifts of selected protons in the [2]rotaxane **4**·4PF$_6$ in various deuterated solvents.

Proton	CD$_3$SOCD$_3$ (300 K)	CD$_3$CN (243 K)	[D$_7$]DMF (223 K)	CD$_3$COCD$_3$ (233 K)
a_1^x	3.29	3.46	3.65	3.62
a_1^y, a_2	6.82	6.75	6.89	6.77
$b_{1'}$	9.52	8.75	9.58	9.31
b_1	9.61	8.88	9.63	9.40
b_2	9.25	8.98	9.87	–
$c_{1'}$	8.49	7.54	8.53	8.08
c_1	8.60	7.73	8.61	8.29
c_2	8.22	7.99	8.94	–
d_1	7.81	7.73	8.11	8.03
d_2	7.88	7.73	8.02	8.03
e_1	5.75	5.55	6.00	6.00
e_2	5.75	5.55	6.15	6.00

Table 4. Relationship between solvent and population of translational isomers **1** and **2** at 300 K.

Solvent	Isomer 1	Isomer 2
CD$_3$SOCD$_3$	67	33
[D$_7$]DMF	71	29
CD$_3$CN	88	12
CD$_3$NO$_2$	93	7
CD$_3$COCD$_3$	100	0

The dynamic properties of this molecular shuttle were investigated by variable-temperature ^{1}H NMR spectroscopy in all the deuterated solvents already mentioned. The fast exchange limit for all the signals capable of undergoing exchange could be obtained in [D$_7$]DMF. In order to calculate an activation energy barrier for process 2, the signals for protons a_1^x and a_1^y were employed as probes. It was not possible to employ the line-broadening method[47] to calculate activation energies for process 2 on account of the coincidence of the signals associated with the triylphenyl groups with those for protons a_1^y and also the signals for protons a_1^x with those for OCH_2 protons. In order to achieve coalescence of the signals arising from protons a_1^x and a_1^y, a field of 270 MHz was used. All other coalescence temperatures (T_c) were obtained with a spectrometer operating at 400 MHz. They are listed in Table 1 along with the limiting chemical shift differences ($\Delta\upsilon$), the rate constants (k_c) at T_c, and the derived activation energy for processes 1 and 2.

The activation energy for process 1 is relatively low in all solvents except CD$_3$SOCD$_3$ considering the steric constraints imposed on such a process by the threaded polyether chain of the dumbbell-shaped component. The shuttling process 2 is associated with a higher activation energy than was observed in

0947-6539/97/0307-1126 $ 17.50+.50/0 Chem. Eur. J. 1997, 3, No. 7

the simple molecular shuttles, for example, $\mathbf{1}\cdot 4PF_6$. This observation is not unreasonable, given the steric constraints to shuttling imposed by the TTF moiety. It is important to note that it is only because of the significant difference in the activation energies between these two processes that they can be measured independently and identified. Although the lower activation energy process 1 was also investigated in other deuterated solvents (Table 1), coalescence of signals associated with a_1^x and a_1^y, corresponding to process 2, was not possible on a high field spectrometer in these solvents as a consequence of their lower boiling points, relative to that of $[D_7]$DMF. In CD_3SOCD_3, the activation energy for process 1 was found to be much larger than those observed in the other solvents; this may result from the much higher viscosity of CD_3SOCD_3. Presumably, process 2 has a similarly elevated activation energy in CD_3SOCD_3 relative to that observed in $[D_7]$DMF. No activation energies for the shuttling process were measured in CD_3NO_2 since the slow exchange limit could not be reached before this solvent froze at $-25\,^{\circ}C$.

UV/Visible Spectroscopy: The complex [TTF·BBIPYBIXYCY][PF_6]$_4$ is green with a charge-transfer band positioned at 854 nm.[20] This band is well separated from the intrinsic absorbances of the TTF nucleus, which "tail" into the visible region. When considering the molecular shuttle $\mathbf{4}\cdot 4PF_6$, the relative population of the TTF-occupied translational isomer, that is, isomer 2, can be derived from the absorbance of the charge-transfer band at $\approx$750 nm (Figure 15). For equimolar solutions of $\mathbf{4}\cdot 4PF_6$ in a variety of solvents, however, comparison of absorbances at this wavelength cannot be relied upon as a direct measurement of the relative TTF occupation, since the extinction coefficient of the charge-transfer band may well vary with solvent. However, integration of the ^{1}H NMR spectra in these solvents provides an absolute measure of the TTF occupation by the cyclophane. Figure 16 shows the relationship between the ^{1}H NMR measurement (see Table 1) and the absorbances of equimolar solutions (0.15 mM) of $\mathbf{4}\cdot 4PF_6$ in these solvents. A reasonable correlation is observed, which implies that the extinction coefficient of the charge-transfer band does not vary significantly in these solvents. In view of this result, the absorbance of $\mathbf{4}\cdot 4PF_6$ in the 600–700 nm region was measured in other solvents that are not commonly available in deuterated forms. These absorbances for equimolar solutions (0.15 mM) have been plotted (Figure 17) against the Kamlet–Taft π-scale of solvent polarisability.[49]

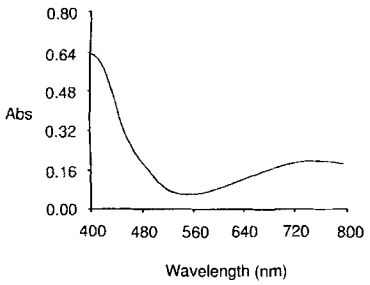

Figure 15. Partial UV/Vis spectrum of the [2]rotaxane $\mathbf{4}\cdot 4PF_6$ in Me_2SO, showing the charge-transfer (CT) band at ca. 750 nm.

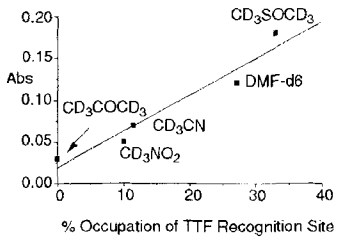

Figure 16. The relationship between absorbance (Abs) of the CT band at 750 nm and the percentage occupation of the translational isomers of the [2]rotaxane $\mathbf{4}\cdot 4PF_6$ determined by integration of the ^{1}H NMR spectra recorded in different solvents at room temprature.

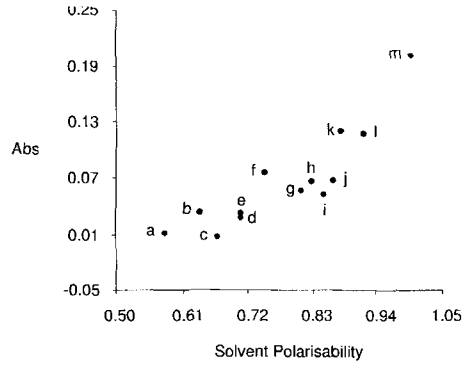

Figure 17. The relationship between absorbance (Abs) of the CT band at 750 nm of the [2]rotaxane $\mathbf{4}\cdot 4PF_6$ and solvent polarizability as determined by the Kamlett–Taft π scale; a = THF; b = hepta-3,5-dione; c = butan-2-one; d = Me_2CO; e = *n*BuCN; f = MeCN; g = 1,2-dichloroethane; h = tetramethylurea; i = $MeNO_2$; j = γ-butyrolactone; k = DMF; l = 1-methyl-2-pyrrolidinone; m = Me_2SO.

Conclusion and Reflections: The general conclusion from this investigation is that enhanced occupation of the TTF site in $\mathbf{4}\cdot 4PF_6$ is favored in more polar solvents, which may be due to the relative contributions of dispersive and electrostatic forces to the binding of the tetracationic cyclophane with the TTF unit and hydroquinone rings. Previous binding studies[20, 22] between the cyclophane and various hydroquinone derivatives have shown that the presence of polyether chains in the substrate is a major factor in determining the magnitude of association constants in these systems. This trend reflects the ability of these polyether chains to interact with the quaternary nitrogen centers on the cyclophane, giving rise to sizable electrostatic contributions, including [C–H···O] hydrogen bonding, to the binding energy. However, in substrates which have a longer aromatic core, such as 4,4′-biphenyl derivatives, the presence of polyether chains has a negligible effect on the binding properties with the tetracationic cyclophane. Presumably, this outcome is a result of the inability of the polyether chains to interact with the bipyridinium rings of the cyclophane in these systems on account of steric factors. Consequently, it is reasonable to assume that electrostatic interactions are not a major contributor to the overall interaction of the cyclophane with the TTF unit. In general, polar solvents will reduce this electrostatic contribution to binding energies by competing more effectively for the solvation of the bipyridinium units. Polar solvents will therefore favor TTF over hydroquinone occupation by reducing the noncovalent bonding interactions in the case of the hydroquinone rings, whilst not particularly affecting the interactions with the TTF unit.

E. Toward Controlling the Shuttling: All three rotaxanes $\mathbf{2}\cdot 4PF_6$, $\mathbf{3}\cdot 4PF_6$, and $\mathbf{4}\cdot 4PF_6$ display rich electrochemistry on account of the redox active character of the π-donor residues in the dumbbell-shaped components and the 4,4′-bipyridinium groups in the cyclophane component. All the studies described in this paper were carried out in MeCN at room temperature with tetrabutyl-

ammonium hexafluorophosphate (0.1 M) as supporting electrolyte. Measurements were made by means of a glassy carbon working electrode, a platinum counter electrode and Ag/AgCl reference electrode. In the discussion, redox couples are quoted vs SCE.

Anodic Window: Analysis of the anodic electrochemical behavior of each rotaxane is aided by comparison with the corresponding polyether species from which the rotaxanes are derived. In the case of rotaxanes **2**·4PF$_6$, **3**·4PF$_6$, and **4**·4PF$_6$, the available anodic window is limited to potentials below 1.5 V vs. SCE due to the irreversible oxidation at ca. 1.6 V of the terminal tritylphenyl residues. The dumbbell-shaped compound **12**, from which **2**·4PF$_6$ is derived, displays a reversible oxidation wave ($E_{1/2}$, 1310 mV vs. SCE), whilst **2**·4PF$_6$ itself displays an analogous redox couple at 1355 mV under the same conditions. In both compounds, the process corresponds to oxidation of a hydroquinone ring. The anodic shift of 45 mV observed for **2**·4PF$_6$ relative to **12** reflects the presence of the positively charged cyclophane in the former species, which discourages the introduction of further positive charges into the assembly. The anodic window of the indole-based [2]rotaxane **3**·4PF$_6$ and the dumbbell-shaped compound **25** from which it is derived show an irreversible oxidation (ca. 1100 mV vs SCE), corresponding to the indole nucleus.

The dumbbell-shaped compound **36** from which the TTF-based [2]rotaxane **4**·4PF$_6$ is derived displays three oxidation waves (Figure 18) corresponding to two successive one-electron

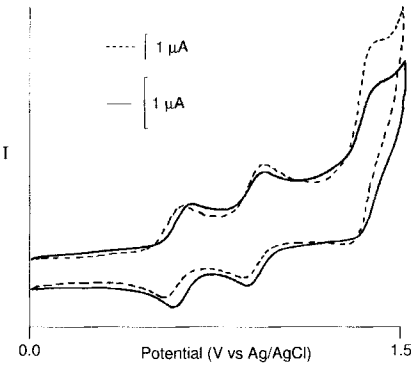

Figure 18. A comparison between the anodic cyclic voltammogram of the dumbbell-shaped compound **36** and the [2]rotaxane **4**·4PF$_6$.

oxidations of the TTF nucleus and a two-electron oxidation of the hydroquinone rings. This description is supported by the comparative current levels for each oxidation wave with the most anodic wave being roughly twice that of the other waves. Comparison of **36** with **4**·4PF$_6$ (Table 5 and Figure 18) indicates that, in the [2]rotaxane, the first oxidation wave of the TTF nucleus is shifted to a more positive potential by 35 mV whilst the second one is shifted by only 5 mV. This observation suggests that the shuttling movement of the cyclophane is hampered by oxidation of the TTF nucleus. Hence, the first TTF-centered oxidation results in an increased energy barrier to the passage of the cyclophane along the thread and thus causes the cyclophane to be effectively tethered at a hydroquinone site. Consequently, the second oxidation wave of the TTF nucleus in

Table 5. Anodic values vs. SCE of the [2]rotaxane **4**·4PF$_6$ and the dumbbell-shaped compound **36**.

Species	E_1 (mV)	E_2 (mV)	E_3 (mV)
4·4PF$_6$	605	900	1330
36	570	895	1325

4·4PF$_6$ is perturbed to a lesser extent than the first, relative to the analogous processes observed in **36**. A similar observation has been made in a chemically and electrochemically controllable molecular shuttle that contains benzidine- and biphenol-derived species as the π-donor residues in the polyether component.[49] Interestingly, in contrast to **36** the third oxidation wave of **4**·4PF$_6$ exhibits less than twice the current level of either of the preceding oxidation waves—an observation which indicates that, in the [2]rotaxane, the cyclophane is forced to occupy a hydroquinone ring after oxidation of the TTF nucleus. It has been shown previously that a hydroquinone ring that is included within the cavity of the cyclophane is oxidized at considerably more positive potentials (>1.5 V) than the free species. Thus, the cyclic voltammogram of **4**·4PF$_6$ provides information about the average position of the cyclophane within the assembly, before, during and after oxidation of the TTF nucleus. The present observation provides a further example, based on the oxidation of a different redox active species, of electrochemically induced control of the shuttling processes in rotaxanes.

Cathodic Window: The cathodic electrochemistry of the rotaxanes is dominated by the reduction of the two bipyridinium units in the macrocyclic tetracationic cyclophane. The parent macrocycle undergoes two consecutive two-electron reductions in MeCN, with $E_{1/2}$ values of −0.296 and −0.734 V vs SCE. The first potential corresponds to the uptake of one electron by each bipyridinium unit in the cyclophane (cyclophane^{4+}/cyclophane^{2+} redox couple), whilst the second potential corresponds to the cyclophane^{2+}/cyclophane couple.

The reduction processes of the cyclophane components of [2]rotaxanes **2**·4PF$_6$, **3**·4PF$_6$, and **4**·4PF$_6$ are more complicated than those described for the parent cyclophane in that, in most cases, both the first and second two-electron reduction waves are resolved into discrete single electron processes, having $\Delta E_{1/2}$ values of <70 mV. It has been shown by Nicholson and Shain[50] that it is possible to determine the half-wave potential for overlapping voltammetric waves in multistep charge-transfer reactions. By using cyclic voltammetry to obtain the peak half-width and the working curves of Myers and Shain,[51] which were later extended by Richardson and Taube,[52] we determined the potential differences between the individual monoelectron reductions of the bisparaquat derivatives. These results are shown in Tables 6 and 7.

The cathodic voltammetric responses of **2**·4PF$_6$, **3**·4PF$_6$, and **4**·4PF$_6$ are shown in Figure 19. The resolution of the simultaneous two-electron processes of the parent cyclophane into overlapping single-electron waves in the [2]rotaxanes may reflect an enhanced degree of communication between the two bipyridinium units of the tetracationic cyclophane as a result of an included π-donor residue within the cyclophane cavity. Alternatively, the observation of single electron waves could conceiv-

0947-6539/97/0307-1128 $ 17.50+.50/0 Chem. Eur. J. 1997, 3, No. 7

Table 6. First reduction waves vs. SCE of the [2]rotaxanes **2**·4PF$_6$, **3**·4PF$_6$, and **4**·4PF$_6$.

[2]Rotaxane	ΔE_p [a] (mV)	$E_p - E_{p/2}$ (mV)	E_p(cath) (mV)	E_1/mV	$E_{1'}$ (mV)
2·4PF$_6$	154	132	−429	−300	−410
3·4PF$_6$	101	90	−285	−200	−270
4·4PF$_6$	70	–	–	−330	–

[a] ΔE_p = peak-to-peak separation of overlapping waves; $E_p - E_{p/2}$ = half-width of two step voltammetric wave; E_p(cath) = most cathodic peak.

Table 7. Second reduction waves vs. SCE of the [2]rotaxanes **2**·4PF$_6$, **3**·4PF$_6$, and **4**·4PF$_6$.

[2]Rotaxane	ΔE_p (mV)	$E_p - E_{p/2}$ (mV)	E_p(cath) (mV)	E_2 (mV)	$E_{2'}$ (mV)
2·4PF$_6$	81	76	−835	−70	−825
3·4PF$_6$	101	86	−712	−630	−700
4·4PF$_6$	143	129	−858	−735	−840

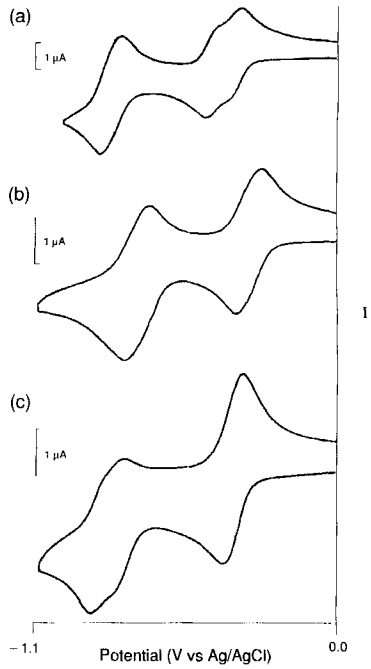

Figure 19. Cathodic cyclic voltammograms of the [2]rotaxanes a) **2**·4PF$_6$, b) **3**·4PF$_6$, and c) **4**·4PF$_6$ illustrating the effects of the dumbbell-shaped components on the reduction of the tetracationic cyclophane in each case.

ably reflect the presence of different cyclophane populations within the rotaxane assembly. This explanation may seem reasonable since two different π-donor sites are present in the dumbbell-shaped component of each rotaxane. However, a similar resolution of the first two-electron reduction wave of the cyclophane has been observed in simple rotaxanes that contain benzidine and *p*-phenylenediamine π-donor groups respectively,[53] but which are unable to display translational isomerism. The observation of resolved redox couples in a host–guest system consisting of a ferrocene-based cryptand, whose redox behavior is responsive to alkali metal ion binding, can be accounted for without invoking kinetic effects.[54] However, this behavior is dependent on a very large binding constant ($\approx 2 \times 10^6\,M^{-1}$) between the host and guest species, whilst the association constants between the tetracationic cyclophane and the various π-donor species present in the dumbbell-shaped components of rotaxanes **2**·4PF$_6$, **3**·4PF$_6$, and **4**·4PF$_6$ are no greater than $10^4\,M^{-1}$. The precise qualities of the included π-donor species that result in enhanced communication between the bipyridinium units in the tetracationic cyclophane are as yet unclear. An explanation has not been found for the significant anodic shifts of the reduction waves associated with **3**·4PF$_6$ relative to the other rotaxanes reported here and, indeed, other rotaxanes described in previous studies.[11]

Conclusions

We have synthesized, by template-directing methods in the final step, and evaluated, by a range of spectroscopic and electrochemical methods, four molecular shuttles in the form of [2]rotaxanes. Variable temperature ^{1}H NMR spectroscopic studies in [D$_7$]DMF of the [2]rotaxane **4**·PF$_6$ (wherein cyclobis(paraquat-*p*-phenylene) is the cyclic component and the polyether chain containing two hydroquinone rings positioned around a tetrathiafulvalene residue and terminated by tetraarylmethane stoppers constitutes the dumbbell component) have established unequivocally the existence of two dynamic processes in this particular system: namely 1) shuttling of the tetracationic cyclophane along the dumbbell-shaped component and 2) rotation of the bipyridinium units of the cyclophane around their long N–N axes. The relative site occupancy of the tetracationic cyclophane on the dumbbell-shaped component of this molecular shuttle shows considerable solvent dependence as revealed by ^{1}H NMR and visible absorption spectroscopy. Moreover, electrochemical control of the shuttling process in the [2]rotaxane has been demonstrated in MeCN at room temperature. Our research on controllable molecular shuttles continues.

Experimental Section

General Methods: Chemicals were purchased from Aldrich and used as received. Solvents and reagents were purified by literature methods where necessary.[55] DMF was distilled from calcium hydride under reduced pressure, MeCN and CH_2Cl_2 were distilled from calcium hydride while tetrahydrofuran (THF) was heated and collected under reflux over Na/benzophenone under nitrogen. NaH was used as a 50% dispersion in mineral oil, which was washed with light petroleum before use. 2-Phenyl-5-hydroxy-1,3-dioxane[56] and [BBIPYXY][PF$_6$]$_2$[11] were prepared according to published procedures. Reactions requiring ultra-high pressure were carried out in Teflon vessels in a custom-built ultra-high pressure reaction vessel, manufactured by PSIKA Pressure Systems Limited (Glossop, UK). Thin-layer chromatography (TLC) was carried out on aluminum or plastic plates, coated with Merck 5735 Kieselgel 60F. Developed plates were dried and scrutinized under a UV lamp. Column chromatography was performed on Kieselgel 60 (0.040–0.063 mm, Merck 9385). Melting points were determined with an Electrothermal 9200 melting point apparatus and are uncorrected. Mass spectra (MS) were recorded on a Kratos Profile spectrometer (EIMS and CIMS) or on a Kratos MS 80 RF spectrometer (FABMS), the latter being equipped with a saddle-field source (Ion Tech) operating at 8 keV with a krypton or xenon primary atom beam in conjunction with a 3-nitrobenzyl alcohol matrix. FAB Mass spectra were recorded in the positive-ion mode at a scan speed of 30 s per decade. Liquid secondary ion mass spectometry (LSIMS) was carried out on a VG-Zab Spec mass spectrometer (accelerating voltage, 8 kV; resolution, 2000). Spectra were recorded in the positive ion mode at a scan speed of 5 s per decade. High resolution mass spectra (LSIMS) were obtained from a VG Zab Spec triple focusing mass spectrometer operating at a resolution of 5000 and voltage scanning with CsI as a reference. ^{1}H NMR spectra were recorded on a Bruker AC 300 (300 MHz) or Bruker AMX 400 (400 MHz) spectrometer (with deuterated solvent as lock and residual solvent or tetramethylsilane as internal reference). ^{13}C NMR spectra were recorded on a Bruker AC 300 (75.5 MHz) or AMX 400 (100 MHz) spectrometer with the JMOD pulse sequence in most cases. Microanalyses were performed by the University of Sheffield Microanalytical Services. The cyclic voltammetry experiments were performed under a purified nitrogen atmosphere. Nitrogen gas was also used to purge all solutions before use. Routinely, a constant concentration of $1 \times 10^{-3}\,M$ of electroactive species was used. The supporting electrolyte was

0.1 M $TBAPF_6$. Measurements were performed with a small (1 mL), single-compartment cell obtained from Cypress Systems (Lawrence, KS). A disk glassy carbon electrode (0.0079 cm^2) and a platinum wire were used as working and counter electrodes, respectively. All potentials ($E_{1/2}$) were determined as the average of the corresponding anodic and cathodic peak potentials.

1,11-Bis{4-[2-(2-(2-(2-hydroxyethoxy)ethoxy)ethoxy)ethoxy]phenoxy}-3,6,9-trioxaundecane (10): A solution of 1,11-bis{4-hydroxyphenoxy}-3,6,9-trioxaundecane **8** (2.04 g, 5.4 mmol) in dry DMF (10 mL) was added over 15 min to a suspension of K_2CO_3 (5.96 g, 43.2 mmol) in DMF (10 mL). The mixture was stirred for 2 h before a solution of **9** (3.64 g, 21.6 mmol) in DMF (10 mL) was added over 15 min. The reaction mixture was stirred at 80 °C for 6 d. After cooling to room temperature, the reaction mixture was filtered, and the solid residue washed with DMF (10 mL). The combined organic extracts were evaporated in vacuo, and the residue was dissolved in CH_2Cl_2 (20 mL), washed with dilute HCl (2 N, 15 mL), and finally with H_2O (2 × 15 mL). The organic phase was dried ($MgSO_4$) and the solvent was evaporated in vacuo. Purification of the residue by column chromatography (SiO_2, 5% MeOH–EtOAc) gave **10** as a white solid (1.87 g, 54%): m.p. 58–61 °C; FABMS: *m/z* 642 (M^+); ^{1}H NMR ($CDCl_3$): δ = 2.83 (brs, 2H), 3.55–3.60 (m, 4H), 3.62–3.75 (m, 20H), 3.76–3.83 (m, 8H), 4.00–4.10 (m, 8H), 6.80 (s, 4H), 6.81 (s, 4H); ^{13}C NMR ($CDCl_3$): δ = 61.9, 62.0, 68.8, 70.4, 71.1, 71.3, 71.4, 116.3, 154.0, 154.1; HRMS calcd for $C_{32}H_{50}O_{13}$ $(M)^+$: 642.3245; found 642.3251.

1,11-Bis{4-[2-(2-(2-(2-triisopropylsilyloxyethoxy)ethoxy)ethoxy)ethoxy]-phenoxy}-3,6,9-trioxaundecane (11): A solution of triisopropylsilyl triflate (2.33 g, 7.29 mmol) in dry CH_2Cl_2 (10 mL) was added over 10 min to a solution of **10** (1.56 g, 2.43 mmol) and imidazole (558 mg, 8.20 mmol) in CH_2Cl_2 (15 mL) cooled to 0–5 °C. The reaction mixture was stirred at room temperature for 2 h and then washed with H_2O (2 × 5 mL). After drying ($MgSO_4$), the solvent was removed in vacuo and the residue was purified by column chromatography (SiO_2, light petroleum then 40% EtOAc–light petroleum) to yield **11** (1.82 g, 78%) as a colorless oil: FABMS: *m/z* 956 (M^+); ^{1}H NMR ($CDCl_3$): δ = 1.00–1.07 (m, 42H), 3.51 (t, 4H, *J* = 5.0 Hz), 3.55–3.62 (m, 16H), 3.72–3.80 (m, 12H), 3.99–4.02 (m, 8H), 6.82 (s, 8H); ^{13}C NMR ($CDCl_3$): δ = 12.0, 14.2, 60.3, 63.0, 68.1, 69.8, 70.7, 70.8, 70.9, 72.8, 115.6, 153.1, 171.0; anal. calcd for $C_{50}H_{90}O_{13}Si_2$: C 62.86, H 9.49; found: C 62.55, H 9.78.

{[2]-[1,11-Bis{4-[2-(2-(2-(2-triisopropylsilyloxyethoxy)ethoxy)ethoxy)ethoxy]-phenoxy}-3,6,9-trioxaundecane][5,12,19,26-tetraazonia[1.0.1.0]paracyclophane]rotaxane}tetrakis(hexafluorophosphate) ({[2]-[11]-[BBIPYBIXYCY]-rotaxane}[PF_6]$_4$, 1·4PF_6): A solution of [BBIPYXY][PF_6]$_2$ (187 mg, 0.26 mmol), 1,4-bis(bromomethyl)benzene (70 mg, 0.26 mmol), **11** (760 mg, 0.79 mmol), and $AgPF_6$ (164 mg, 0.65 mmol) in dry MeCN (10 mL) was stirred at room temperature in the dark for 7 d. The mixture was centrifuged to remove the precipitate (AgBr), and after decantation the solvent was evaporated and the residue suspended in CH_2Cl_2 (3 × 10 mL), being centrifuged each time. The organic extracts were evaporated in vacuo and the residue washed several times with Et_2O. The residue was then purified by column chromatography [SiO_2, MeOH/2 N NH_4Cl/$MeNO_2$ (7:2:1)]. The rotaxane-containing fractions were combined and evaporated in vacuo without heating. The residue was partitioned between $MeNO_2$ (10 mL) and H_2O (5 mL), and saturated aqueous NH_4PF_6 (5 mL) was added. The organic phase was washed with saturated aqueous NH_4PF_6 (2 × 5 mL). The solvent was removed in vacuo without heating, and the residue was suspended in H_2O (2 × 5 mL), then MeOH (2 × 5 mL), and finally dried to yield 1·4PF_6 as a red solid (172 mg, 32%); m.p. > 280 °C; FABMS: *m/z* 1910 $(M - PF_6)^+$, 1765 $(M - 2PF_6)^+$; ^{1}H NMR (CD_3CN) at 293 K: δ = 1.00–1.05 (m, 42H), 3.58–3.65 (m, 8H), 3.68–3.88 (m, 32H), 5.69 (s, 8H), 7.75 (d, 8H, *J* = 7.0 Hz), 7.77 (s, 8H), 8.90 (d, 8H, *J* = 7.0 Hz); ^{13}C NMR (CD_3COCD_3): δ = 12.6, 18.3, 63.8, 65.6, 68.1, 70.6, 71.2, 71.4, 71.6, 73.4, 126.8, 131.8, 137.7, 145.7, 147.4; HRMS calcd for $C_{86}H_{122}N_4O_{13}F_{18}Si_2P_3$ $(M - PF_6)^+$: 1909.7472; found 1909.7497; calcd for $C_{86}H_{122}N_4O_{13}F_{12}Si_2P_2$ $(M - 2PF_6)^+$: 1764.7831; found 1764.7936.

1-{2-(2-(2-Hydroxyethoxy)ethoxy)ethoxy}-4-{2-(2-(2-*tert*-butyldimethylsilyloxyethoxy)ethoxy)ethoxy)}benzene (15): A solution of *tert*-butyldimethylsilyl chloride (0.5 g, 3.34 mmol) in DMF (10 mL) was added over 10 min to a solution of **5** (1.0 g, 2.67 mmol) and imidazole (0.45 g, 6.7 mmol) in DMF (10 mL) cooled to 0–5 °C. The reaction mixture was stirred at room temperature for 3 h and the DMF then removed in vacuo at 90 °C. The residue was extracted into CH_2Cl_2 (20 mL) and washed with H_2O (3 × 5 mL). After drying ($MgSO_4$), the solvent was removed, and the residue washed with cold light petroleum (4 × 5 mL). Further purification was achieved by column chromatography (SiO_2, 50% EtOAc/CH_2Cl_2) to yield **15** (0.5 g, 38%) as a colorless oil; FABMS: *m/z* 488 (M^+); ^{1}H NMR ($CDCl_3$): δ = 0.07 (s, 6H), 0.89 (s, 9H), 2.50 (brs, 1H), 3.54–3.79 (m, 16H), 3.81–3.87 (m, 4H), 4.05–4.12 (m, 4H), 6.84 (s, 4H); ^{13}C NMR ($CDCl_3$): δ = −5.3, 18.3, 25.9, 61.6, 62.7, 68.0, 69.8, 70.3, 70.7, 70.8, 72.6, 115.6, 153.0, 153.2; anal. calcd for $C_{24}H_{48}O_8Si$: C, 58.50; H, 9.82; found: C, 58.68; H, 9.22.

1-{2-(2-(2-*tert*-Butyldimethylsiloxyethoxy)ethoxy)ethoxy}-4-{2-(2-(2-(toluene-*p*-sulphonyloxy)ethoxy)ethoxy)ethoxy}benzene (16): A solution of tosyl chloride (4.0 g, 21 mmol) in CH_2Cl_2 (30 mL) was added over 15 min to a stirred solution at 0 °C of **15** (8.1 g, 16.6 mmol), Et_3N (5.0 g, 49.8 mmol) and DMAP (50 mg, 0.04 mmol) in CH_2Cl_2 (80 mL). After standing at 4 °C for 15 h, the reaction mixture was poured onto ice and then extracted with dilute aqueous HCl (3 N, 2 × 10 mL) and H_2O (2 × 10 mL). The organic phase was dried ($MgSO_4$) and the solvent removed. Column chromatography (SiO_2, 50% light petroleum/$CHCl_3$, then $CHCl_3$) afforded **16** as a colorless oil (8.95 g, 84%); FABMS: *m/z* 642 (M^+); ^{1}H NMR ($CDCl_3$): δ = 0.06 (s, 6H), 0.91 (s, 9H), 2.43 (s, 3H), 3.55–3.86 (m, 18H), 3.97–4.04 (m, 4H), 4.08–4.12 (m, 2H), 6.84 (s, 4H), 7.34 (d, 2H, *J* = 8.0 Hz), 7.81 (d, 2H, *J* = 8.0 Hz); ^{13}C NMR ($CDCl_3$): δ = −5.2, 18.4, 21.6, 25.9, 62.7, 68.1, 68.8, 69.3, 69.9, 70.7, 70.8, 73.0, 115.6, 128.0, 129.8, 133.1, 144.8, 153.1, anal. calcd for $C_{31}H_{50}O_{10}SSi$: C 57.92, H 7.84, S 4.99; found: C 57.61, H 7.72, S 5.10.

1-{2-(2-(2-(4-Tritylphenoxy)ethoxy)ethoxy)ethoxy}-4-{2-(2-(2-hydroxyethoxy)ethoxy)ethoxy}benzene (13): A solution of **16** (10.8 g, 17.5 mmol) in DMF (30 mL) was added to a vigorously stirred mixture of tritylphenol (5.0 g, 14.9 mmol) and anhydrous K_2CO_3 (5.1 g, 36.9 mmol) in DMF (40 mL) at 70 °C. The reaction mixture was stirred at 70 °C for 96 h before being filtered and reduced in vacuo. The residue was extracted into CH_2Cl_2 (50 mL) and washed with a saturated aqueous NaCl solution (3 × 20 mL), followed by H_2O (2 × 20 mL). The organic phase was then dried ($MgSO_4$) and the solvent removed in vacuo. The residue was taken up into NBu_4F in THF (1 M, 20 mL) and the solution stirred for 3 h. The solvent was then removed in vacuo and the residue taken up into CH_2Cl_2 (30 mL) and washed with H_2O (3 × 15 mL). After drying ($MgSO_4$), the solvent was removed in vacuo, and the crude oil purified by column chromatography (SiO_2, EtOAc) to yield **13** as a white solid (5.12 g, 44%); m.p. 88–89 °C; FABMS: *m/z* 692 (M^+); ^{1}H NMR ($CDCl_3$): δ = 2.43 (brs, 1H), 3.65–3.78 (m, 12H), 3.80–3.91 (m, 6H), 4.03–4.16 (m, 6H), 6.79 (d, 2H, *J* = 9.0 Hz), 6.83 (s, 4H), 7.10 (d, 2H, *J* = 9.0 Hz), 7.14–7.24 (m, 15H); ^{13}C NMR ($CDCl_3$): δ = 61.8, 64.3, 67.3, 68.1, 69.8, 69.9, 70.4, 70.8, 72.5, 113.4, 115.6, 125.9, 127.4, 131.1, 132.2, 139.2, 147.1, 153.1, 153.2, 156.8, anal. calcd for $C_{43}H_{48}O_8$: C 74.54, H 6.98; found: C 74.27, H 7.07.

1,4-Bis{1-(2-(2-hydroxyethoxy)ethoxy)ethoxy}methyl}benzene (18): Sodium metal (2.54 g, 110.2 mmol) was dissolved in triethylene glycol (150 mL) at 40 °C. 1,4-Bis(bromomethyl)benzene (14.5 g, 55.1 mmol) was then added as a solid and the mixture stirred and heated at 40 °C for 30 h before H_2O (150 mL) was added. This mixture was extracted with CH_2Cl_2 (4 × 100 mL), the combined organic extracts dried ($MgSO_4$), and the solvent removed in vacuo. The residue was purified by column chromatography (SiO_2, 50% Me_2CO/CH_2Cl_2) to yield **18** as a colorless oil (13.5 g, 60%); FABMS: *m/z* 402 (M^+); ^{1}H NMR ($CDCl_3$): δ = 3.00 (t, 2H, *J* = 6.5 Hz), 3.50–3.70 (m, 24H), 4.48 (s, 4H), 7.28 (s, 4H); ^{13}C NMR ($CDCl_3$): δ = 61.4, 69.3, 70.2, 70.4, 70.5, 72.6, 72.9, 127.8, 137.4; HRMS calcd for $C_{20}H_{35}O_8$ $(M + H)^+$: 403.2349; found 403.2331.

1-{1-(2-(2-(2-Hydroxyethoxy)ethoxy)ethoxy)methyl}-4-{1-(2-(2-(2-*tert*-butyldimethylsiloxyethoxy)ethoxy)ethoxy)methyl}benzene (19): The monosilyl ether **19** was prepared in 41% yield from **18**, employing a procedure similar to that described for **15**. White solid; m.p. 56–58 °C; MS: *m/z* 516 (M^+); ^{1}H NMR ($CDCl_3$): δ = 0.07 (s, 6H), 0.89 (s, 9H), 2.60 (brt, 1H), 3.54–3.80 (m, 24H), 4.55 (s, 4H), 7.31 (s, 4H); ^{13}C NMR ($CDCl_3$): δ = −5.3, 18.3, 25.9, 61.6, 62.7, 69.3, 69.4, 70.3, 70.6, 70.7, 72.6, 72.7, 73.0, 127.8, 137.5, 137.7; anal calcd for $C_{26}H_{48}O_8Si$: C 58.50, H 9.82; found: C 58.68, H 9.22; HRMS calcd for $C_{26}H_{49}O_8Si$ $(M + H)^+$: 517.3197; found 517.3194.

0947-6539/97/0307-1130 $ 17.50+.50/0 Chem. Eur. J. 1997, 3, No. 7

1-{1-(2-(2-(2-(Toluene-*p*-sulphonyloxy)ethoxy)ethoxy)ethoxy)methyl}-4-{1-2-(2-(2-*tert*-butyldimethylsiloxyethoxy)ethoxy)ethoxy)methyl}benzene (20): The tosylate **20** was prepared in 62% yield from **19**, employing a procedure similar to that described for **16**. Colorless oil; MS: *m/z* 670 (M^+); ^{1}H NMR ($CDCl_3$): δ = 0.07 (s, 6H),0.89 (s, 9H), 2.44 (s, 3H), 3.53–3.71 (m, 20H), 3.77 (t, 2H, J = 4.5 Hz), 4.15 (t, 2H, J = 4.5 Hz), 4.54 (s, 2H), 4.56 (s, 2H), 7.31 (s, 4H), 7.33 (d, 2H, J = 8.0 Hz), 7.80 (d, 2H, J = 8.0 Hz); ^{13}C NMR ($CDCl_3$): δ = −5.2, 18.4, 21.6, 26.0, 62.7, 68.7, 69.3, 69.4, 70.6, 70.7, 72.7, 73.0, 127.8, 128.0, 129.8, 130.3, 133.1, 137.6, 137.7, 144.8.

1-{1-(2-(2-(2-Hydroxyethoxy)ethoxy)ethoxy)methyl}-4-{1-(2-(2-(2-(4-trityl-phenoxy)ethoxy)ethoxy)ethoxy)methyl}benzene (14): The alcohol **14** was prepared in 56% yield from **20**, employing a procedure similar to that described for **13**. White solid; m.p. 38–39 °C; FABMS: *m/z* 720 (M^+); ^{1}H NMR ($CDCl_3$): δ = 2.51 (1H, bt, J = 5.0 Hz), 3.60–3.77 (m, 20H), 3.85 (t, 2H, J = 5.0 Hz), 4.10 (t, 2H, J = 5.0 Hz), 4.46 (s, 4H), 6.79 (d, 2H, J = 8.5 Hz), 7.09 (d, 2H, J = 8.5 Hz), 7.19–7.25 (m, 15H), 7.31 (s, 4H); ^{13}C NMR ($CDCl_3$): δ = 61.7, 64.3, 67.3, 69.4, 69.5, 69.8, 70.4, 70.6, 70.7, 70.8, 72.6, 73.0, 113.4, 115.36, 125.9, 127.4, 127.9, 129.9, 131.2, 132.2, 137.5, 137.8, 139.2, 147.1, 156.8; HRMS calcd for $C_{45}H_{52}O_8$ (M)$^+$: 720.3662; found 720.3668; anal. calcd $C_{45}H_{52}O_8$: C 74.97, H 7.27; found: C 74.52, H 7.22.

1-{1-(2-(2-(2-(Toluene-*p*-sulphonyloxy)ethoxy)ethoxy)ethoxy)methyl}-4-{1-(2-(2-(2-(4-tritylphenoxy)ethoxy)ethoxy)ethoxy)methyl}benzene (17): The tosylate **17** was prepared in 74% yield from **14**, employing a procedure similar to that described for **16**, chromatography ($CHCl_3$/EtOAc; 9:1). White solid; FABMS: *m/z* 874 (M^+); ^{1}H NMR ($CDCl_3$): δ = 2.43 (s, 3H), 3.59–3.79 (m, 18H), 3.84 (t, 2H, J = 6.0 Hz), 4.15 (t, 2H, J = 6.0 Hz), 4.09 (t, 2H, J = 6.0 Hz), 4.53 (s, 2H), 4.56 (s, 2H), 6.79 (d, 2H, J = 8.5 Hz), 7.09 (d, 2H, J = 8.5 Hz), 7.14–7.34 (m, 21H), 7.79 (d, 2H, J = 8.0 Hz); ^{13}C NMR ($CDCl_3$): δ = 21.6, 53.4, 64.3, 67.3, 68.7, 69.2, 69.4, 69.5, 69.8, 70.6, 70.7, 70.8, 70.9, 73.0, 113.4, 125.8, 127.4, 127.8, 128.0, 129.8, 131.1, 132.2, 133.1, 137.6, 137.7, 139.1, 144.7, 147.0, 156.8; anal. calcd for $C_{52}H_{58}O_{10}S$: C 71.37, H 6.68; found: C 71.08, H 6.78.

1-{4-[1-(2-(2-(2-(4-Tritylphenoxy)ethoxy)ethoxy)ethoxy)phenoxy}-17-{4-[(2-(2-(2-(4-tritylphenoxy)ethoxy)ethoxy)ethoxy)methyl]phenylmethoxy}-3,6,9,12,15-pentaoxaheptadecane (12): A solution of **13** (0.53 g, 0.76 mmol) in dry THF (5 mL) was added dropwise to a stirred suspension of NaH (54 mg, 50% in mineral oil, washed previously with light petroleum, 1.13 mmol) in refluxing dry THF (5 mL) under nitrogen. The mixture was refluxed for 2 h before a solution of **17** (0.67 g, 0.76 mmol) in dry THF (5 mL) was added dropwise. The mixture was heated under reflux for a further 16 h before being cooled to room temperature. Excess of NaH was quenched by addition of a few drops of H_2O, and the solvent then removed in vacuo and the residue partitioned between CH_2Cl_2 (20 mL) and H_2O (10 mL). The organic phase was washed with dilute HCl (2 N, 10 mL) and H_2O (10 mL), dried ($MgSO_4$), and then concentrated in vacuo. The residue was washed with hot EtOH (3 × 10 mL) and then recrystallised from Et_2O to afford **12** as a white solid (0.84 g, 78%); m.p. 62–63 °C; FABMS: *m/z* 1395 (M^+); ^{1}H NMR (CD_3COCD_3): δ = 3.55–3.66 (m, 32H), 3.74–3.81 (m, 8H), 4.00–4.05 (m, 4H), 4.07–4.11 (m, 4H), 4.49 (s, 2H), 4.50 (s, 2H), 6.82–6.87 (m, 8H), 7.08 (d, 4H, J = 8.0 Hz), 7.16–7.28 (m, 30H), 7.30 (s, 4H); ^{13}C NMR ($CDCl_3$): δ = 64.4, 67.4, 68.1, 69.3, 69.5, 69.8, 70.0, 70.5, 70.7, 70.9, 73.0, 113.5, 115.7, 125.9, 127.5, 127.9, 131.2, 132.2, 137.7, 137.8, 139.2, 147.1, 153.2, 156.8; anal. calcd for $C_{88}H_{98}O_{15}$: C 75.72, H 7.08; found: C 75.60, H 7.04.

{[2]-[1-{4-[1-(2-(2-(2-(4-Tritylphenoxy)ethoxy)ethoxy)ethoxy)phenoxy}-17-{4-[(2-(2-(2-(4-tritylphenoxy)ethoxy)ethoxy)ethoxy)methyl]phenylmethoxy}-3,6,9,12,15-pentaoxaheptadecane][5,12,19,26-tetraazonia[1.0.1.0]paracyclophane]rotaxane} tetrakis(hexafluorophosphate) ({[2]-[12][BBIPYBIXYCY]-rotaxane}[PF_6]$_4$, 2·4PF_6): A solution of [BBIPYXY][PF_6]$_2$ (0.59 g, 0.84 mmol), 1,4-bis(bromomethyl)benzene (0.22 g, 0.84 mmol), the dumbbell-shaped component **12** (2.50 g, 1.79 mmol), and $AgPF_6$ (0.53 g, 2.09 mmol) in dry MeCN (20 mL) was stirred at room temperature in the dark for 7 d. The orange solution was filtered to remove the precipitate (AgBr) and the solvent was then removed in vacuo. The residue was dissolved in THF (30 mL) and insoluble material removed by centrifugation. After decantation, the solvent was removed in vacuo. The residue was dissolved in EtOAc (30 mL) to which Et_2O (10 mL) was then added. On standing overnight a red solid precipitated, which was removed by filtration. The filtered material was dissolved in Me_2CO (1 mL) and purified by column chromatography (SiO_2, MeOH/$MeNO_2$/sat. aq. NH_4PF_6 (32:7:1). The rotaxane-containing fractions were combined and evaporated in vacuo without heating. The residue was partitioned between EtOAc (10 mL) and H_2O (5 mL). The organic phase was washed with H_2O (2 × 5 mL) and Et_2O added dropwise until the onset of turbidity. On standing overnight a red precipitate was formed, which was separated by centrifugation and dried under vacuum (0.5 mbar, 70 °C, 15 h) to afford **2**·4PF_6 as an orange solid (162 mg, 8%); m.p. > 280 °C; FABMS: *m/z* 2350 ($M - PF_6$)$^+$, 2205 ($M - 2PF_6$)$^+$, 2060 ($M - 3PF_6$)$^+$; ^{1}H NMR (CD_3CN, at 233 K: δ = 2.82–4.11 (m, 52H), 4.45 (d, 2.8H), 5.50–5.75 (m, 8H), 6.08–6.29 (2d, 2H), 6.63–7.11 (m, 7.2H), 7.11–8.37 (m, 34H), 8.38–8.83 (m, 16H), 8.50–8.76 (2d, 4H), 8.83–8.94 (2d, 4H); ^{13}C NMR (CD_3CN): δ = 52.2, 55.3, 65.7, 68.3, 70.2, 70.6, 70.8, 71.2, 71.3, 71.6, 114.2, 114.3, 126.9, 127.2, 128.7, 131.6, 131.7, 132.8, 137.8, 145.6, 147.3, 148.2, 148.3; HRMS calcd for $C_{124}H_{130}N_4O_{15}F_{18}P_3$ ($M - PF_6$)$^+$: 2349.8458; found 2349.8543; calcd for $C_{124}H_{130}N_4O_{15}F_{12}P_2$ ($M - 2PF_6$)$^+$: 2204.8816; found 2204.8851; anal. calcd for $C_{124}H_{130}N_4O_{15}P_4F_{24}$: C 59.66, H 5.25, N 2.24; found: C 59.36, H 5.02, N 2.19.

4-Benzyloxy-(*N*-*tert*-butoxycarbonyl)phenylhydrazine (30): To a solution of 4-benzyloxyphenylhydrazine[57] **29** (2.75 g, 11.0 mmol) and Et_3N (2.22 g, 22.0 mmol) in MeOH (30 mL) was added di-(*tert*-butyl)dicarbonate (2.6 g, 12 mmol). The mixture was heated under reflux for 1 h and cooled to room temperature. The solid materials were removed by filtration and the filtrate reduced. The residue was washed with light petroleum (3 × 15 mL) and H_2O (3 × 15 mL), then dried ($MgSO_4$). The solid was then recrystallized from hexane to afford **30** as a white solid (1.55 g, 45%); m.p. 97–99 °C; MS: *m/z* 314 (M^+); ^{1}H NMR ($CDCl_3$): δ = 1.47 (s, 9H), 5.02 (s, 2H), 6.80 (d, 2H, J_{AB} 9.5 Hz), 6.91 (d, 2H, J_{AB} 9.5 Hz), 7.30–7.42 (m, 5H); ^{13}C NMR ($CDCl_3$): δ = 28.3, 70.6, 81.1, 114.6, 115.8, 127.5, 127.8, 127.9, 128.6, 137.4, 142.5, 153.5, 156.4, anal. calcd for $C_{18}H_{22}N_2O_3$: C 68.77, H 7.05, N 8.91; found: C 68.64, H 6.81, N 8.51.

4-Hydroxy-*N*-(*tert*-butoxycarbonyl)phenylhydrazine (31): A solution of **30** (1.50 g, 4.7 mmol) in EtOH (200 mL) was subjected to hydrogenolysis (10% Pd/C, 500 mg) at room temperature for 4 h. After filtration (Celite), the filtrate was concentrated to leave a solid residue, which was washed with Et_2O (3 × 10 mL) to yield **31** as a white solid (0.92 g, 91%); m.p. 167–168 °C (decomp.); MS: *m/z* 224 (M^+); ^{1}H NMR ($CDCl_3$): δ = 1.51 (brs, 9H), 6.39 (brs, 1H), 6.76 (d, 2H), 7.18 (d, 2H); ^{13}C NMR ($CDCl_3$): δ = 28.3, 70.6, 81.1, 114.6, 115.8, 127.5, 127.8, 128.5, 128.6, 137.4, 142.5, 153.5, 156.4; HRMS calcd for $C_{11}H_{16}N_2O_3$ (M)$^+$: 224.1161; found 224.1162.

2-(2-(2-(4-Tritylphenoxy)ethoxy)ethoxy)ethanol (32): A mixture of 4-tritylphenol (30 g, 89 mmol), chloroethoxyethoxyethanol (**9**, 30 g, 178 mmol), and anhydrous K_2CO_3 (30 g, 217 mmol) in DMF (250 mL) was stirred at 70 °C for 48 h. The reaction mixture was cooled to room temperature and filtered, and the solvent removed in vacuo. The residue was partitioned between CH_2Cl_2 (200 mL) and H_2O (200 mL). The organic phase was separated and washed with dilute HCl (2 N, 2 × 100 mL), H_2O (2 × 100 mL), dried ($MgSO_4$), and then the solvent removed. The residue was recrystallized from CH_2Cl_2/light petroleum to afford **32** as a white solid (37 g, 89%); m.p. 116–118 °C; ^{1}H NMR ($CDCl_3$): δ = 2.00 (brs, 1H), 3.59–3.63 (m, 2H), 3.66–3.75 (m, 6H), 3.83–3.87 (m, 2H), 4.08–4.13 (m, 2H), 6.79 (d, 2H, J_{AB} = 8.5 Hz), 7.09 (d, 2H, J_{AB} = 8.5 Hz), 7.14–7.28 (m, 15H); ^{13}C NMR ($CDCl_3$): δ = 61.8, 64.4, 67.3, 69.8, 70.4, 70.8, 72.6, 113.4, 125.9, 127.5, 131.2, 132.2, 139.3, 147.1, 156.7; HRMS calcd for $C_{31}H_{32}O_4$ (M)$^+$: 468.2301; found 468.2323.

2-(2-(2-(4-Tritylphenoxy)ethoxy)ethoxy)ethyl 4-Methylbenzenesulfonate (33): The tosylate **33** was prepared in 66% yield from **32**, employing a procedure similar to that described for **16**. White solid; m.p. 86–88 °C; MS: *m/z* 622 (M^+); ^{1}H NMR ($CDCl_3$): δ = 2.37 (s, 3H), 3.55–3.71 (m, 6H), 3.76–3.83 (m, 2H), 4.03–4.09 (m, 2H), 4.10–4.17 (m, 2H), 6.75 (d, 2H, J_{AB} = 8.5 Hz), 7.08 (d, 2H, J_{AB} = 8.0 Hz), 7.13–7.25 (m, 15H), 7.29 (d, 2H, J_{AB} = 8.0 Hz), 7.78 (d, 2H, J_{AB} = 8.5 Hz); ^{13}C NMR ($CDCl_3$): δ = 21.6, 64.4, 67.3, 68.8, 69.3, 69.8, 70.8, 113.4, 125.9, 127.4, 128.0, 129.8, 131.1, 132.2, 133.1, 139.3, 144.8, 147.0, 156.7, anal. calcd for $C_{38}H_{38}O_6S$: C 73.29, H 6.15; found: C 73.18, H 6.17.

4-{2-(2-(2-(4-Tritylphenoxy)ethoxy)ethoxy)ethoxy}-(*N*-*tert*-butoxycarbonyl)-phenylhydrazine (26): To a vigorously stirred mixture of **31** (0.80 g, 3.6 mmol) and K_2CO_3 (1.00 g, 7.2 mmol) in dry DMF (15 mL) was added **33** (2.22 g, 3.6 mmol) in dry DMF (10 mL) and the mixture heated at 60 °C for 60 h. The reaction mixture was cooled to room temperature and filtered. The solvent was removed in vacuo and the residue was partitioned between CH_2Cl_2 (50 mL) and H_2O (50 mL). The organic phase was washed with 5% aqueous K_2CO_3 (2 × 25 mL) and H_2O (3 × 25 mL), dried ($MgSO_4$), and then concentrated. The residue was purified by column chromatography (SiO_2, EtOAc/light petroleum) to afford **26** as a white solid (1.11 g, 46%); m.p. 87–90 °C; FABMS: *m/z* 674 (M^+); ^{1}H NMR ($CDCl_3$): δ = 1.45 (brs, 9H), 3.74 (s, 4H), 3.80–3.88 (m, 4H), 4.04–4.12 (m, 4H), 6.74–6.84 (m, 6H), 7.09 (d, 2H, J = 8.5 Hz), 7.14–7.28 (m, 15H); ^{13}C NMR ($CDCl_3$): δ = 28.3, 64.3, 67.3, 68.0, 69.8, 69.9, 70.8, 81.1, 113.4, 114.5, 115.6, 125.8, 127.4, 131.1, 132.2, 139.1, 142.4, 147.0, 153.5, 156.3, 156.7; anal. calcd for $C_{42}H_{46}N_2O_6$: C 74.75, H 6.87, N 4.15; found: C 74.63, H 6.60, N 4.12.

14-{4-(2-(2-(2-(4-Tritylphenoxy)ethoxy)ethoxy)ethoxy)phenoxy}-6,9,12-trioxatetradecan-2-one ethylene acetal (27): The acetal **27** was prepared in 51% yield from **13** (3.12 g, 4.5 mmol), 5-chloro-2-pentanone ethylene acetal **34** (3.0 g, 18 mmol) and NaH (0.33 g, 50% in mineral oil, washed previously with light petroleum, 6.75 mmol), employing a procedure similar to that described for **12**. White solid; m.p. 63–66 °C; FABMS: *m/z* 820 (M^+); ^{1}H NMR ($CDCl_3$): δ = 1.31 (s, 3H), 1.66–1.72 (m, 4H), 3.45–3.49 (m, 2H), 3.56–3.75 (m, 12H), 3.79–3.87 (m, 6H), 3.89–3.94 (m, 4H), 4.04–4.12 (m, 6H), 6.78 (d, 2H, J = 8.5 Hz), 7.09 (d, 2H, J = 8.5 Hz), 6.83 (s, 4H), 7.14–7.27 (m, 15H); ^{13}C NMR ($CDCl_3$): δ = 23.9, 24.3, 35.6, 64.3, 64.6, 67.3, 68.1, 69.8, 69.9, 70.1, 70.7, 70.9, 71.4, 110.0, 113.4, 115.6, 125.8, 127.4, 131.1, 132.2, 139.2, 147.0, 153.1, 156.7; HRMS calcd for $C_{50}H_{60}O_{10}$: 843.4084; found 843.4080; anal. calcd for $C_{50}H_{60}O_{10}Na$ $(M + Na)^+$: C 73.15, H 7.37; found: C 72.95, H 6.97.

1-{2-Methyl-5-[2-(2-(2-(4-tritylphenoxy)ethoxy)ethoxy)ethoxy]-3-indenyl}-11-{4-(2-(2-(2-(4-tritylphenoxy)ethoxy)ethoxy)ethoxy)phenoxy}-3,6,9-trioxa-undecane (25): To a suspension of **26** (750 mg, 1.13 mmol) in a mixture of EtOH/H_2O (1:1, 40 mL) was added dilute HCl (2 N, 11 mL) and the resultant solution then heated under reflux for 1 h under nitrogen. A solution of **27** (930 mg, 1.13 mmol), warmed to 85 °C in EtOH (40 mL), was added dropwise and the reaction mixture refluxed for 18 h. Upon cooling the reaction mixture, a brown oil separated and solidified on standing. The solid was filtered and purified by column chromatography (SiO_2, EtOAc/light petroleum) to afford **25** as an off-white solid (0.75 g, 51%); m.p. 79–81 °C; FABMS: *m/z* 1316 (M^+); ^{1}H NMR ($CDCl_3$): δ = 2.37 (s, 3H), 2.97 (t, 2H, J = 7.0 Hz), 3.55–3.90 (m, 26H), 4.01–4.19 (m, 12H), 6.74–6.84 (m, 10H), 6.97 (d, 1H, J = 8.5 Hz), 7.04–7.11 (m, 6H), 7.14–7.28 (m, 28H), 7.69 (brs, 1H); ^{13}C NMR ($CDCl_3$): δ = 11.9, 25.0, 29.8, 64.4, 67.4, 68.2, 68.6, 69.9, 70.0, 70.2, 70.4, 70.7, 70.8, 70.9, 71.5, 102.1, 108.1, 110.9, 111.2, 113.5, 115.7, 126.0, 127.5, 129.3, 130.6, 131.3, 132.3, 132.9, 139.2, 147.1, 153.2, 156.8.

{[2]-[1-{2-Methyl-5-[2-(2-(2-(4-tritylphenoxy)ethoxy)ethoxy)ethoxy]-3-indenyl}-11-{4-(2-(2-(2-(4-tritylphenoxy)ethoxy)ethoxy)ethoxy)phenoxy}-3,6,9-trioxaundecane][5,12,19,26-tetraazonia-[1.0.1.0]-paracyclophane]rotaxane} tetrakis(hexafluorophosphate) ({[2]-[25][BBIPYBIXY]rotaxane}[PF_6]$_4$, 3·4PF_6): A solution of [BBIPYXY][PF_6]$_2$ (0.37 g, 0.53 mmol), BBB (0.14 g, 0.53 mmol), the dumbbell-shaped component **25** (0.70 g, 0.53 mmol), and $AgPF_6$ (0.33 g, 1.33 mmol) in dry MeCN (7 mL) was stirred at room temperature in the dark for 7 d. The [2]rotaxane **3**·4PF_6 was purified by a procedure similar to that described for **2**·4PF_6 to yield a purple solid (115 mg, 9%); m.p. > 280 °C; FABMS: *m/z* 2271 $(M - PF_6)^+$; ^{1}H NMR (CD_3CN) at 298 K: δ = 2.13 (s, 3H), 2.45 (t, 2H), 3.37 (brt, 2H), 3.43 (brs, 4H), 3.51–3.57 (m, 6H), 3.58–3.78 (m, 10H), 3.81–3.98 (m, 12H), 4.01–4.08 (m, 8H), 5.53–5.62 (m, 8H), 6.46 (d, 2H), 6.51 (brm, 1H), 6.75 (d, 2H), 6.88 (d, 1H), 6.99 (d, 2H), 7.09 (d, 2H), 7.14–7.28 (m, 31H), 7.60 (d, 8H), 7.73 (s, 8H), 8.59 (brs, 1H), 8.76 (d, 8H); HRMS calcd for $C_{121}H_{121}N_5O_{12}F_{18}P_3$ $(M - PF_6)^+$: 2270.7937; found 2270.7840; anal. calcd for $C_{121}H_{121}N_5O_{12}P_4F_{24}\cdot 2H_2O$: C 59.23, H 4.93, N 2.85; found: C 59.20, H 4.81, N 2.76.

2-Phenyl-5-[2-(*tert*-butoxy)-2-oxoethoxy]-1,3-dioxane (38a,b): 2-Phenyl-5-hydroxy-1,3-dioxane **37a,b** (5 g, as a mixture of diastereoisomers, 27.7 mmol), NaOH (10 g), *t*-butylbromoacetate (12.6 g, 69 mmol), and Et_4NBr (5.8 g, 27.7 mmol) were partitioned between H_2O (20 mL) and PhMe (20 mL) and the mixture stirred very vigorously for 12 h at room temperature. The reaction mixture was then diluted with H_2O (40 mL) and PhMe (20 mL) and the organic phase subsequently washed with H_2O (3 × 40 mL) and dried ($MgSO_4$), and the solvent removed in vacuo. The residue was purified by column chromatography (SiO_2, EtOAc/light petroleum; 1:2) in order to separate the two diastereoisomers of 2-phenyl-5-*tert*-butylacetyloxy-1,3-dioxane (**38a,b**). Both compounds were obtained as crystalline solids to give a combined yield of (3.91 g, 48%). The *trans*-isomer **38a** was employed in all subsequent reactions; m.p. 64–65 °C; MS: *m/z* 294 (M^+); ^{1}H NMR ($CDCl_3$): δ = 1.48 (s, 9H), 3.61–3.78 (m, 3H), 4.05 (s, 2H), 4.41–4.49 (m, 2H), 5.41 (s, 1H), 7.33–7.40 (m, 3H), 7.45–7.52 (m, 2H); ^{13}C NMR ($CDCl_3$): δ = 28.1, 67.7, 69.6, 69.9, 82.1, 101.3, 126.1, 128.3, 129.0, 137.6, 169.3; anal. calcd for $C_{16}H_{22}O_5$: C 65.29, H 7.53; found: C 65.39, H 7.64.

***trans*-2-Phenyl-5-(2-hydroxyethoxy)-1,3-dioxane (39a)**: A solution of $LiAlH_4$ (70 mg, 1.84 mmol) in dry THF (10 mL) was added dropwise to a stirred solution of *trans*-2-phenyl-5-[2-(*tert*-butoxy)-2-oxoethoxy]-1,3-dioxane **38a** (1.0 g, 3.3 mmol) in dry THF (10 mL) at room temperature, under nitrogen, and the mixture then heated under reflux for 4 h Thereafter, the reaction mixture was cooled to room temperature and quenched by the addition of EtOAc (1 mL) followed by H_2O (1 mL). The resulting precipitate was removed by filtration and the filtrate concentrated in vacuo to leave a residue which was dissolved in CH_2Cl_2 (20 mL), washed with H_2O (2 × 10 mL), dried ($MgSO_4$), and the solvent removed to afford *trans*-2-phenyl-5-(2-hydroxyethoxy)-1,3-dioxane **39a** as a white crystalline solid (0.61 g, 80%); m.p. 45–46 °C; MS: *m/z* 224 (M^+); ^{1}H NMR ($CDCl_3$): δ = 1.96 (brs, 1H), 3.57–3.80 (m, 7H), 4.35–4.46 (m, 2H), 5.41 (s, 1H), 7.30–7.41 (m, 3H), 7.43–7.51 (m, 2H); ^{13}C NMR ($CDCl_3$): δ = 61.8, 68.8, 70.0, 70.9, 101.3, 126.2, 128.3, 129.0, 137.7; anal. calcd for $C_{12}H_{16}O_4$: C 64.27, H 7.19; found: C 64.39, H 7.23.

***trans*-2-Phenyl-5-[2-(4-methylbenzenesulfonyloxy)]-1,3-dioxane (40a)**: The tosylate *trans*-2-phenyl-5-[2-(4-methylbenzenesulfonyloxy)]-1,3-dioxane **40a** was prepared in 89% yield from *trans*-2-phenyl-5-(2-hydroxyethoxy)-1,3-dioxane **39a** by a procedure similar to that described for **16**. White crystalline solid; m.p. 92.5 °C; MS: *m/z* 378 (M^+); ^{1}H NMR ($CDCl_3$); δ = 2.46 (s, 3H), 3.41–3.78 (m, 5H), 4.07–4.19 (m, 2H), 4.21–4.35 (m, 2H), 5.38 (s, 1H), 7.27–7.51 (m, 7H), 7.80 (d, 2H, J = 8.5 Hz); ^{13}C NMR ($CDCl_3$): δ = 21.7, 67.2, 69.0, 69.1, 69.8, 101.3, 126.1, 128.0, 128.3, 129.1, 129.9, 133.0, 137.5, 145.0, anal. calcd for $C_{19}H_{22}O_6S$: C 60.30, H 5.86; found: C 60.32, H 5.73.

***trans*-2-Phenyl-5-{2-(2-(2-(4-(2-(2-(2-(4-tritylphenoxy)ethoxy)ethoxy)-ethoxy)phenoxy)ethoxy)ethoxy)ethoxy}-1,3-dioxane (41)**: Compound **41** was prepared as a white solid (750 mg, 97%) from **13** (600 mg, 0.86 mmol), *trans*-2-phenyl-5-[2-(4-methylbenzenesulfonyloxy)]-1,3-dioxane (**40a**, 330 mg, 0.86 mmol), and NaH (48 mg, 50% suspension in oil, previously washed with light petroleum, 0.95 mmol) by a procedure similar to that described for **12**; m.p. 81–82 °C; FABMS: *m/z* 898 (M^+); ^{1}H NMR ($CDCl_3$): δ = 3.59–3.75 (m, 19H), 3.79–3.87 (m, 6H), 3.93–4.12 (m, 6H), 4.35–4.43 (m, 2H), 5.38 (s, 1H), 6.78 (d, 2H, J = 9.0 Hz), 6.82 (s, 4H), 7.08 (m, 2H), 7.14–7.25 (m, 15H), 7.31–7.39 (m, 3H), 7.43–7.49 (m, 2H); ^{13}C NMR ($CDCl_3$): δ = 67.3, 68.1, 69.0, 69.3, 69.8, 69.9, 70.2, 70.7, 70.8, 70.9, 101.3, 113.4, 115.6, 125.9, 126.1, 127.5, 128.3, 129.0, 131.2, 132.2, 137.8, 139.2, 147.1, 153.2, 156.8. Anal. calcd for $C_{55}H_{62}O_{11}$: C 73.47, H 6.95; found: C 73.59, H 6.85.

2-Hydroxymethyl-14-{4-(2-(2-(2-(4-tritylphenoxy)ethoxy)ethoxy)ethoxy)-phenoxy}-3,6,9,12-tetraoxatetradecanol (42): A solution of **41** (700 mg, 0.78 mmol) and concentrated sulfuric acid (2 mL) in EtOH (100 mL) was refluxed for 2 h. The reaction mixture was then cooled, neutralized by the addition of a saturated aqueous sodium hydrogencarbonate solution, and the solvent removed in vacuo. The residue was taken up into CH_2Cl_2 (40 mL) and washed with H_2O (3 × 40 mL), dried ($MgSO_4$), and concentrated in vacuo to afford **42** as a colorless oil, which solidified on standing (450 mg, 71%); m.p. 58–60 °C; FABMS: *m/z* 810 (M^+); ^{1}H NMR ($CDCl_3$): δ = 1.96 (brs, 2H), 3.48–3.54 (m, 1H), 3.58–3.77 (m, 18H), 3.78–3.89 (m, 8H), 3.93–4.13 (m, 6H), 6.78 (d, 2H, J = 8.5 Hz), 6.83 (s, 4H), 7.09 (d, 2H, J = 8.5 Hz), 7.14–7.25 (m, 15H); ^{13}C NMR ($CDCl_3$): δ = 62.5, 67.3, 68.1, 69.4, 69.8, 69.9, 70.5, 70.6, 70.8, 70.9, 81.3, 113.4, 115.6, 125.9, 127.4, 131.1, 132.2, 139.2, 147.1, 153.2, 156.7; anal. calcd for $C_{48}H_{58}O_{11}$: C 71.09, H 7.21; found: C 70.96, H 7.36.

0947-6539/97/0307-1132 $ 17.50+.50/0 Chem. Eur. J. 1997, 3, No. 7

2-(4-Methylbenzenesulfonyloxy)methyl-14-{4-(2-(2-(4-tritylphenoxy)-ethoxy)ethoxy)ethoxy)phenoxy}-3,6,9,12-tetraoxatetradecyl 4-methylbenzenesulfonate (43): The ditosylate **43** was prepared in 94% yield from **42**, employing a procedure similar to that described for **16**. White solid; m.p. 45–47 °C; FABMS: *m/z* 1118 (M^+); ^{1}H NMR ($CDCl_3$): δ = 2.44 (s, 6H), 3.47–3.74 (m, 16H), 3.77–3.87 (m, 7H), 4.00–4.13 (m, 10H), 6.78 (d, 2H, J = 9.0 Hz), 6.82 (s, 4H), 7.09 (d, 2H, J = 9.0 Hz), 7.14–7.25 (m, 15H), 7.34 (d, 4H, J = 8.0 Hz), 7.74 (d, 4H, J = 8.0 Hz); ^{13}C NMR ($CDCl_3$): δ = 62.5, 64.3, 67.3, 68.1, 69.4, 69.8, 69.9, 70.5, 70.6, 70.8, 70.9, 81.3, 113.4, 115.6, 125.9, 127.4, 131.1, 132.2, 139.2, 147.0, 153.2, 156.7; anal. calcd for $C_{62}H_{70}O_{15}S_2$: C 66.53, H 6.30, S 5.73; found: C 66.63, H 6.49, S 5.6.

Thione precursor 44: A solution of NaOMe (made by dissolving sodium metal (138 mg, 6 mmol) in dry 50% C_6H_6/MeOH (10 mL) was added dropwise to a stirred solution of dibenzoyl-4,5-dithio-1,3-dithiole-2-thione (1.11 g, 2.73 mmol) in dry 50% C_6H_6/MeOH (10 mL), and the mixture stirred for 30 min. A solution of **43** (3.06 g, 2.73 mmol) in a dry 50% C_6H_6/MeOH mixture (15 mL) was then added dropwise, and the mixture heated under reflux for 3 h. After cooling, the reaction mixture was concentrated in vacuo to leave a residue, which was purified by column chromatography (SiO_2, EtOAc/light petroleum). The desired thione **44** was obtained as a bright yellow oil (2.10 g, 81%); FABMS: *m/z* 972 (M^+); ^{1}H NMR ($CDCl_3$): δ = 2.52–2.65 (m, 2H), 3.05 (d, 1H, J = 2.5 Hz), 3.11 (d, 1H, J = 2.5 Hz), 3.60–3.75 (m, 16H), 3.79–3.87 (m, 6H), 3.94 (br m, 1H), 4.04–4.12 (m, 6H), 6.78 (d, 2H, J = 9.0 Hz), 6.82 (s, 4H), 7.09 (d, 2H, J = 9.0 Hz), 7.13–7.25 (m, 15H); ^{13}C NMR ($CDCl_3$): δ = 36.7, 67.3, 68.1, 69.3, 69.8, 69.9, 70.7, 70.9, 113.4, 115.6, 125.9, 127.4, 131.2, 132.2, 139.2, 147.1, 156.2, 156.7; anal. calcd for $C_{51}H_{56}O_9S_5$: C 62.93, H 5.80, S 16.47; found: C 62.98, H 5.64, S 16.70.

Ketone 35: A solution of mercury(II) acetate (1.75 g, 5.4 mmol) in glacial acetic acid (70 mL) was added to a solution of **44** (2.1 g, 21.5 mmol) in $CHCl_3$ (50 mL) and the mixture stirred for 30 min at room temperature. The resulting precipitate (HgS) was separated by centrifugation and the supernatant then diluted with $CHCl_3$ (80 mL), before being washed with saturated aqueous $NaHCO_3$ (2 × 100 mL) and H_2O (100 mL). The organic phase was dried ($MgSO_4$) and the solvent removed to afford the ketone **35** as a pale yellow oil (1.85 g, 89%); FABMS: *m/z* 956 (M^+); ^{1}H NMR ($CDCl_3$): δ = 2.51–2.67 (m, 2H), 3.02 (d, 1H, J = 2.5 Hz), 3.08 (d, 1H, J = 2.5 Hz), 3.60–3.75 (m, 16H), 3.87–3.79 (m, 6H), 3.92 (br m, 1H), 4.03–4.13 (m, 6H), 6.78 (d, 2H, J = 8.5 Hz), 6.82 (s, 4H), 7.09 (d, 2H, J = 8.5 Hz), 7.14–7.25 (m, 15H); ^{13}C NMR ($CDCl_3$): δ = 36.7, 64.3, 67.3, 69.2, 69.8, 69.9, 70.7, 70.9, 113.4, 115.6, 125.9, 127.4, 131.1, 132.2, 139.2, 147.1, 152.2, 156.8; anal. calcd for $C_{51}H_{56}O_{10}S_4$: C 63.99, H 5.90, S 13.40; found: C 64.17, H 5.96, S 13.30.

Dumbbell-shaped compound 36: A solution of **35** (1.80 g, 1.88 mmol) in freshly distilled Et_3P (15 mL) was heated at 115 °C for 2 h under nitrogen. The reaction mixture was cooled to room temperature and diluted with light petroleum (20 mL). On standing overnight, an orange oil separated and was isolated by decanting the solvent layer. The oil was washed with hot Et_2O (3 × 20 mL) and hot EtOH (3 × 20 mL) and dried in vacuo to afford component **36** as an orange oil (1.02 g, 58%); FABMS: *m/z* 1881 (M^+); ^{1}H NMR ($CDCl_3$): δ = 2.32–2.65 (m, 4H), 2.85–3.00 (m, 4H), 3.56–3.78 (m, 32H), 3.80–3.90 (m, 14H), 4.02–4.14 (m, 12H), 6.78 (d, 4H, J = 8.5 Hz), 6.82 (s, 8H), 7.08 (d, 4H, J = 8.5 Hz), 7.14–7.25 (m, 30H); ^{13}C NMR ($CDCl_3$): δ = 36.7, 64.3, 67.3, 68.1, 69.0, 69.8, 69.9, 70.7, 70.9, 113.4, 115.6, 125.9, 127.4, 131.1, 132.2, 139.2, 147.1, 153.1, 156.8; anal. calcd for $C_{102}H_{112}O_{18}S_8$: C 65.08, H 6.00, S 13.63; found: C 64.82, H 5.85, S 13.80.

{[2]-[36][5,12,19,26-Tetraazonia-[1.0.1.0]paracyclophane]rotaxane} tetrakis-(hexafluorophosphate) ({[2]-[36][BBIPYBIXYCY]rotaxane}[PF_6]$_4$, 4·4PF_6): A solution of the dumbbell-shaped component **36** (327 mg, 0.174 mmol), [BBIPYXY][PF_6]$_2$ (122 mg, 0.174 mmol), and 1,4-bis(bromomethyl)benzene (45 mg, 0.174 mmol) in dry DMF (8 mL) was transferred to a Teflon tube and compressed (9 kbar) at room temperature for 96 h. The solvent was then removed in vacuo at 60 °C and the residue suspended in EtOAc (10 mL). Insoluble rotaxane-containing materials were removed by filtration and then dissolved in DMF containing 5% saturated aqueous NH_4PF_6 (4 mL). Addition of H_2O (4 mL) precipitated the hexafluorophosphate salts, which were removed by filtration, washed with MeOH (10 mL) and then extracted with EtOAc (10 mL). Upon standing, the rotaxane **4**·4PF_6 crystallized from the EtOAc solution as small orange crystals (43 mg, 8%); m.p. >280 °C; FABMS: *m/z* 2836 ($M - PF_6$)$^+$, 2690 ($M - 2PF_6$)$^+$, 2545 ($M - 3PF_6$)$^+$; ^{1}H NMR (CD_3COCD_3) at 298 K: δ = 2.61–2.38 (br m, 4H), 2.90 (d, 2H), 3.06 (d, 2H), 4.03–3.48 (m, 58H), 4.09 (t, 2H), 4.18 (m, 2H), 6.05 (s, 8H), 6.57 (d, 2H), 6.85–6.82 (m, 6H), 6.95 (d, 2H), 7.07 (d, 2H), 7.28–7.12 (m, 30H), 8.06 (s, 8H), 8.23 (d, 8H), 9.35 (d, 8H); ^{13}C NMR [$(CD_3)_2$NCDO]: δ = 64.9, 68.1, 68.6, 70.1, 70.2, 70.6, 70.9, 71.1, 71.3, 71.5, 113.6, 113.9, 114.1, 116.1, 118.1, 126.6, 125.7, 127.4, 128.3, 131.2, 131.4, 131.6, 132.5, 137.8, 145.8, 146.4, 147.7, 153.8; HRMS calcd for $C_{138}H_{144}N_4O_{18}F_{18}P_3S_8$ ($M - PF_6$)$^+$: 2835.7167; found 2835.7214.

X-ray crystal structure data for [BBIPYBIXYCY·2MIN][PF_6]$_4$: $C_{44}H_{44}N_5 \cdot 4PF_6 \cdot 2CH_3CN$, M = 1301.81, monoclinic, a = 10.940(2), b = 19.846(4), c = 14.000(3) Å, β = 110.46(3)°, V = 2847.9(10) Å^3, space group $P2_1/n$, Z = 2, $\mu(Cu_{K\alpha})$ = 2.320 mm^{-1}, ρ_c = 1.518 g cm^{-3}, $F(000)$ = 1320. 3842 independent reflections ($2\theta < 114°$), 2527 observed reflections $|F_o| > 4\sigma|F_o|$. The data were collected on a Siemens P4PC diffractometer with $Cu_{K\alpha}$ radiation and ω scans. The structure was solved by direct methods; full-matrix least-squares refinement with all non-hydrogen atoms anisotropic gave R_1 = 0.1082 and wR_1 = 0.2444. The 2-methylindole molecule is disordered about a center of symmetry with additional rotational disorder. Because the position of the indole nitrogen cannot be uniquely identified, the C_2-related nitrogen and carbon atoms were refined as partial occupancies for C and N superimposed species. One of the PF_6 anions is also disordered and was split into two orientations with an occupancy of 0.5. Hydrogen atoms were assigned idealised positions with fixed isotropic U and were allowed to ride on their parent atoms. Crystallographic data (excluding structure factors) for the structure reported in this paper have been deposited with the Cambridge Crystallographic Data Centre as supplementary publication no. CCDC-100195. Copies of the data can be obtained free of charge on application to The Director, CCDC, 12 Union Road, Cambridge CB2 1EZ, UK (Fax: Int. code +(1223)336-033; e-mail: deposit@chemcrys.cam.ac.uk). For data for [BBIPYBIXYCY·TTF][PF_6]$_4$ see ref. [39].

Acknowledgements: The research was supported by the Engineering and Physical Sciences Research Council and the Wolfson Foundation in the United Kingdom. A NATO Collaborative Research Grant (to A. E. K. and N. S.) helped support work carried out at the University of Miami (by R. A. B.). For postdoctoral fellowship support, we thank the Ciba-Geigy Foundation for the Promotion of Science in Japan (on behalf of M. A.), the Deutsche Forschungsgemeinschaft (on behalf of G. M.), and the Ramsay Memorial Trust (on behalf of S. J. L.).

Received: August 21, 1996 [F446]

[1] a) F. L. Carter, R. E. Siatkowsky, H. Woltjien, *Molecular Electronic Devices*, Elsevier, Amsterdam, **1988**; b) Special Section: Engineering a Small World, *Science*, **1991**, *254*, 1300–1342; c) K. E. Drexler, *Engines of Creation*, Fourth Estate, London, **1990**; d) K. E. Drexler, *Nanosystems, Molecular Machinery, Manufacturing and Computation*, Wiley, New York, **1992**; e) K. E. Drexler, *Annu. Rev. Biophys. Biomol. Struct.* **1994**, *23*, 377–405.

[2] a) J. S. Lindsey, *New J. Chem.* **1991**, *15*, 153–180; b) D. Philp, J. F. Stoddart, *Synlett*, **1991**, 445–458; c) G. M. Whitesides, J. P. Mathias, C. T. Seto, *Science*, **1991**, *254*, 1312–1319; d) G. M. Whitesides, E. E. Simanek, J. P. Mathias, C. T. Seto, D. N. Chin, M. Mammen, D. M. Gordon, *Acc. Chem. Res.* **1995**, *28*, 37–44; e) D. Philp, J. F. Stoddart, *Angew. Chem. Int. Ed. Engl.* **1996**, *35*, 1154–1196.

[3] a) H. Ringsdorf, B. Schlarb, J. Venzmer, *Angew. Chem. Int. Ed. Engl.* **1988**, *27*, 113–158; b) W. Muller, H. Ringsdorf, E. Rump, G. Wildburg, X. Zhang, L. Angermaier, W. Knoll, M. Liley, J. Spinke, *Science* **1993**, *262*, 1706–1708.

[4] The following group of references (refs. [5–7]) is by no means exhaustive. They have been included to demonstrate that the functioning aspect of supramolecular chemistry is as varied as the components used.

[5] a) J.-M. Lehn, *Angew. Chem. Int. Ed. Engl.* **1990**, *29*, 1304–1319; b) S. H. Kawai, S. L. Gilat, J.-M. Lehn, *J. Chem. Soc. Chem. Commun.* **1994**, 1011–1013; c) A. Livoreil, C. O. Dietrich-Buchecker, J.-P. Sauvage, *J. Am. Chem. Soc.* **1994**, *116*, 9399–9400; d) M. J. Marsella, P. J. Carrol, T. M. Swager, *J. Am. Chem. Soc.* **1994**, *116*, 9347–9348; e) Q. Zhou, T. M. Swager, *ibid.* **1995**, *117*, 7017–7018.

[6] a) J. F. Stoddart, *Chem. Aust.* **1992**, *59*, 576–577; b) R. Ballardini, V. Balzani, M. T. Gandolfi, L. Prodi, M. Venturi, D. Philp, H. G. Ricketts, J. F. Stoddart, *Angew. Chem. Int. Ed. Engl.* **1993**, *32*, 1301–1303; c) P. R. Ashton, R. Ballardini, V. Balzani, M. T. Gandolfi, D. J.-F. Marquis, L. Pérez-Garcia, L. Prodi, J. F. Stoddart, M. Venturi, *J. Chem. Soc. Chem. Commun.* **1994**, 177–180; d) J. A. Preece, J. F. Stoddart, in *The Ultimate Limits of Fabrication and Mea-*

surement (Ed.: M. Welland), Kluwer, Dordrecht, **1995**, 1–8; e) A. C. Benniston, A. Harriman, V. M. Lynch, *J. Am. Chem. Soc.* **1995**, *117*, 5275–5291; f) P. R. Ashton, R. Ballardini, V. Balzani, A. Credi, M. T. Gandolfi, S. Menzer, L. Pérez-García, L. Prodi, J. F. Stoddart, M. Venturi, A. J. P. White, D. J. Williams, *ibid.* **1995**, *117*, 11171–11197; g) R. Ballardini, V. Balzani, A. Credi, M. T. Gandolfi, S. J. Langford, S. Menzer, L. Prodi, J. F. Stoddart, M. Venturi, D. J. Williams, *Angew. Chem. Int. Ed. Engl.* **1996**, *35*, 978–981; h) A. Credi, V. Balzani, S. J. Langford, J. F. Stoddart, *J. Am. Chem. Soc.* **1997**, *119*, 2679–2681.

[7] a) B. L. Feringa, W. F. Jager, B. de Lange, *J. Am. Chem. Soc.* **1991**, *113*, 5468–5470; b) R. A. Bissell, A. P. de Silva, H. Q. M. Gunaratne, P. L. M. Lynch, G. E. M. Maguire, K. R. A. Sandanayake, *Chem. Rev. Soc.* **1992**, *21*, 187–195; c) B. L. Feringa, W. F. Jager, B. de Lange, *Tetrahedron*, **1993**, *49*, 8267–8310; d) M. Jorgensen, K. Lerstrup, P. Frederikson, T. Bjornholm, P. Sommer-Larsen, K. Schaumberg, K. Brunfeldt, J. Bechgaard, *J. Org. Chem.* **1993**, *58*, 2785–2790; e) T. R. Kelly, M. C. Bowyer, K. V. Bhaskar, D. Bebbington, A. Garcia, F. Lang, M. H. Kim, M. P. Jette, *J. Am. Chem. Soc.* **1994**, *116*, 3657–3658; f) D. H. Vance, A. W. Czarnik, *ibid.* **1994**, *116*, 9397–9398; g) P. J. Clapp, B. Armitage, P. Roosa, D. F. Obrien, *ibid.* **1994**, *116*, 9166–9173; h) G. Wenz, *Angew. Chem. Int. Ed. Engl.* **1994**, 803–822; i) S. Hanessian, M. Simond, S. Roelens, *J. Am. Chem. Soc.* **1995**, *117*, 7630–7645; j) T. D. James, K. R. A. S. Sandanayake, R. Iguchi, S. Shinkai, *ibid.* **1995**, *117*, 8982–8987; k) R. G. Chapman, J. C. Sleman, *ibid.* **1995**, *117*, 9081–9082.

[8] a) D. B. Amabilino, J. F. Stoddart, *New Scientist* **1994**, *141, No. 1913, 19 Feb*, 25–29; b) D. B. Amabilino, C. O. Dietrich-Bucheker, A. Livoreil, L. Pérez-García, J.-P. Sauvage, J. F. Stoddart, *J. Am. Chem. Soc.* **1996**, *118*, 3905–3913.

[9] a) C. O. Dietrich-Buchecker, J.-P. Sauvage, J. P. Kitzinger, *Tetrahedron Lett.* **1983**, *24*, 5095–5098; b) J. P. Sauvage, *Acc. Chem. Res.* **1990**, *23*, 319–327; c) C. O. Dietrich-Buchecker, J.-P. Sauvage, in *Supramolecular Chemistry*, Kluwer, Amsterdam, **1992**, pp. 259–277; d) D. B. Amabilino, J. F. Stoddart, *Chem. Rev.* **1995**, *95*, 2725–2828.

[10] a) P. R. Ashton, T. T. Goodnow, A. E. Kaifer, M. Reddington, A. M. Z. Slawin, N. Spencer, J. F. Stoddart, C. Vicent, D. J. Williams, *Angew. Chem. Int. Ed. Engl.* **1989**, *28*, 1396–1399; b) C. L. Brown, D. Philp, J. F. Stoddart, *Synlett.* **1991**, 459–461.

[11] P. L. Anelli, P. R. Ashton, R. Ballardini, V. Balzani, M. Delgado, M. T. Gandolfi, T. T. Goodnow, A. E. Kaifer, D. Philp, M. Pietraszkiewicz, L. Prodi, M. V. Reddington, A. M. Z. Slawin, N. Spencer, J. F. Stoddart, C. Vicent, D. J. Williams, *J. Am. Chem. Soc.* **1992**, *114*, 193–218.

[12] P. R. Ashton, D. Philp, N. Spencer, J. F. Stoddart, *J. Chem. Soc. Chem. Commun.* **1992**, 1125–1128.

[13] a) D. B. Amabilino, J. F. Stoddart, *Pure Appl. Chem.* **1993**, *65*, 2351–2359; P. R. Ashton, M. Belohradsky, D. Philp, J. F. Stoddart, *J. Chem. Soc. Chem. Commun.* **1993**, 1269–1274; b) P. R. Ashton, M. Belohradsky, D. Philp, J. F. Stoddart, *ibid.* **1993**, 1274–1277; c) P. R. Ashton, R. Ballardini, V. Balzani, M. Belohradsky, M. T. Gandolfi, D. Philp, L. Prodi, F. M. Raymo, M. V. Reddington, N. Spencer, J. F. Stoddart, M. Venturi, D. J. Williams, *J. Am. Chem. Soc.* **1996**, *118*, 4931–4951; d) M. Asakawa, P. R. Ashton, R. Ballardini, V. Balzani, M. Belohradsky, M. T. Gandolfi, O. Kocian, L. Prodi, F. M. Raymo, J. F. Stoddart, M. Venturi, *ibid.* **1997**, *119*, 302–310.

[14] The term rotaxane comes from the Latin *axis* meaning axle and *rota* for wheel. For more information, see G. Schill, *Catenanes, Rotaxanes, and Knots*, Academic Press, New York, **1971**. The numbers in the brackets immediately preceding the name *rotaxane* indicate the number of constituent components present within the complex. Hence, a [2]rotaxane is made up of two components, that is, *one* dumbbell-shaped compound and *one* wheel.
For rotaxanes based principally on hydrogen bonding for their self-assembly, see: a) F. Vögtle, M. Händel, S. Meier, S. Ottens-Hildebrandt, F. Ott, T. Schmidt, *Liebegs Ann. Chem.* **1995**, 739–745; b) F. Vögtle, T. Dünnwald, M. Händel, R. Jäger, S. Meier, G. Harder, *Chem. Eur. J.* **1996**, *2*, 640–643; c) F. Vögtle, R. Jäger, M. Händel, S. Ottens-Hildebrandt, W. Schmidt, *Synthesis* **1996**, 353–356; d) F. Vögtle, F. Ahuis, S. Baumann, J. Sessler, *Liebigs Ann. Chem.* **1996**, 921–926; e) R. Jäger, M. Händel, J. Harren, K. Rissanen, F. Vögtle, *ibid.* **1996**, 1201–1207; f) F. Vögtle, R. Jäger, M. Händel, S. Ottens-Hildebrandt, *Pure Appl. Chem.* **1996**, *68*, 225–232; g) A. G. Kolchinski, D. H. Busch, N. W. Alcock, *J. Chem. Soc. Chem. Commun.* **1995**, 1289–1291; h) P. R. Ashton, P. T. Glink, J. F. Stoddart, P. R. Tasker, A. J. P. White, D. J. Williams, *Chem. Eur. J.* **1996**, *2*, 729–736; i) P. R. Ashton, P. T. Glink, J. F. Stoddart, S. Menzer, P. R. Tasker, A. J. P. White, D. J. Williams, *Tetrahedron Lett.* **1996**, *37*, 6217–6220.
For cyclodextrin-based rotaxanes, see: a) A. Harada, J. Li, M. Kamachi, *Nature (London)* **1992**, *356*, 325–327; **1994**, *370*, 126–128; *J. Am. Chem. Soc.* **1994**, *116*, 3192–3196; b) G. Wenz, B. Keller, *Angew. Chem. Int. Ed. Engl.* **1992**, *31*, 197–199; c) M. Born, H. Ritter, *ibid.* **1995**, *34*, 309–311.
For polyrotaxanes, see: a) H. W. Gibson, S. Wu, P. R. Lecavalier, C. Wu, Y. X. Shen, *J. Am. Chem. Soc.* **1995**, *117*, 852–874; b) I. Yamaguchi, K. Osakada, T. Yamamoto, *ibid.* **1996**, *118*, 1811–1812; c) J.-M. Kern, J.-P. Sauvage, G. Bidan, M. Billon, B. Divisia-Blohorn, *Adv. Mater.* **1996**, *8*, 580–582.
For rotaxanes incorporating transition-metal ions, see: a) C. Wu, P. R. Lecavalier, Y. X. Shen, H. W. Gibson, *Chem. Mater.* **1991**, *3*, 569–572; J.-C. Chambron, V. Heitz, J.-P. Sauvage, *J. Chem. Soc. Chem. Commun.* **1992**, 1131–1133; *J. Am. Chem. Soc.* **1993**, *115*, 12378–12384; c) J.-C. Chambron, A. Harriman, V. Heitz, J.-P. Sauvage, *ibid.* **1993**, *115*, 6109–6114 and 7419–7425; d) F. Diederich, C. O. Dietrich-Buchecker, J.-F. Nierengarten, J.-P. Sauvage, *J. Chem. Soc. Chem. Commun.* **1995**, 781–782; e) N. Solladié, J.-C. Chambron, C. O. Dietrich-Buchecker, J.-P. Sauvage, *Angew. Chem. Int. Ed. Engl.* **1996**, *35*, 906–909.

[15] P. L. Anelli, N. Spencer, J. F. Stoddart, *J. Am. Chem. Soc.* **1991**, *113*, 5131–5133.

[16] P. R. Ashton, R. A. Bissell, N. Spencer, J. F. Stoddart, M. S. Tolley, *Synlett* **1992**, 914–918.

[17] P. R. Ashton, R. A. Bissell, R. Górski, D. Philp, N. Spencer, J. F. Stoddart, M. S. Tolley, *Synlett* **1992**, 919–922.

[18] P. R. Ashton, R. A. Bissell, N. Spencer, J. F. Stoddart, M. S. Tolley, *Synlett* **1992**, 923–926.

[19] R. A. Bissell, J. F. Stoddart, in *Computations for the Nano-Scale. NATO ASI Series Vol. 240* (Eds.: P. E. Blöchl, A. J. Fisher, C. Joachim), Kluwer, Dordrecht, **1993**, pp. 141–152.

[20] a) B. Odell, M. V. Reddington, A. M. Z. Slawin, N. Spencer, J. F. Stoddart, D. J. Williams, *Angew. Chem. Int. Ed. Engl.* **1988**, *27*, 1547–1550; b) P. R. Ashton, B. Odell, M. V. Reddington, A. M. Z. Slawin, J. F. Stoddart, D. J. Williams, *ibid.* **1988**, *27*, 1550–1553; c) M. Asakawa, W. Dehaen, G. L'abbé, S. Menzer, J. Nouwen, F. M. Raymo, J. F. Stoddart, D. J. Williams, *J. Org. Chem.* **1996**, *61*, 9591–9595 and references cited therein.

[21] It will be convenient, in presenting these results, to employ simple acronyms composed of letters and occasionally numbers to identify the neutral and charged compounds displayed in the schemes and figures. Thus, 1,4-bis(bromomethyl)benzene is abbreviated to BBB and bisparaphenylene-34-crown-10 to BPP34C10. The other acronyms employed can be deduced on the basis of the following definitions: CY, XY, and BIXY represent cyclophane, xylyl, and bisxylyl units, respectively. The [2]rotaxanes have been named by a combination of the acronyms of their two components, for example, {[2]-[BPP34C10]-[BIPYBIXYDAPCY]rotaxane}$[PF_6]_4$.

[22] C. L. Brown, D. Philp, J. F. Stoddart, *Synlett* **1991**, 462–464. The term threading relates to the inclusion of a linear molecule inside an already formed macrocyclic component. Clipping relates to the self-assembly process in which the macrocycle is formed around the linear component—in essence, a template-directed synthesis.

[23] a) D. B. Amabilino, P. R. Ashton, G. R. Brown, W. Hayes, J. F. Stoddart, M. S. Tolley, D. J. Williams, *J. Chem. Soc. Chem. Commun.* **1994**, 2475–2478; b) P. R. Ashton, L. Pérez-García, J. F. Stoddart, A. J. P. White, D. J. Williams, *Angew. Chem. Int. Ed. Engl.* **1995**, *34*, 571–574.

[24] D. B. Amabilino, P. R. Ashton, C. L. Brown, E. Córdova, L. A. Godinez, T. T. Goodnow, A. E. Kaifer, S. P. Newton, M. Pietraszkiewicz, D. Philp, F. M. Raymo, A. S. Reder, M. T. Rutland, A. M. Z. Slawin, N. Spencer, J. F. Stoddart, D. J. Williams, *J. Am. Chem. Soc.* **1995**, *117*, 1271–1293.

[25] In the absence of $AgPF_6$, yields of the [2]rotaxane are lower because of precipitation of the intermediates as their Br^- salts.

[26] Positive-ion FABMS revealed two characteristic peaks at *m/z* 1910 and 1765, corresponding to the loss of one and two hexafluorophosphate counterions, respectively, from **1**·4PF6.

[27] These δ values relate to a region in the ^{1}H NMR spectrum where the resonances of the protons on the two hydroquinone rings might be expected to occur.

[28] E. S. Pysh, N. C. Yang, *J. Am. Chem. Soc.* **1963**, *85*, 2124–2130. Replacement of two methyl groups in *p*-xylene with *O*-methylene groups would be expected to raise the oxidation potential of this aromatic residue.

[29] The diol **18** may be prepared in 60% yield from the reaction of the monosodium salt of triethyleneglycol with 1,4-bis(bromomethyl)benzene.

[30] As a result of the symmetrical nature of the degenerate [2]rotaxane **1**·4PF_6, we are unable to differentiate between exchange processes 1 and 2 in the coalescence of the bipyridinium signals. We do note, however, that there is a significant variation in the activation energy barriers (12.4–13.2 kcal mol^{-1}) calculated for **1**·4PF_6 using various ^{1}H NMR probes (Table 1). This observation may reflect the operation of two different exchange processes with very similar activation energy barriers.

[31] We did not observe a sidedness in the *para*-phenylene rings of the tetracationic cyclophane components in **2**·4PF_6, **3**·4PF_6, or **4**·4PF_6 at low temperature. Hence, these protons are not differentiated into primed and unprimed signals.

[32] It was not possible to calculate energy barriers for processes 1 and 2 from the variable temperature ^{1}H NMR spectra of the signals for g_1, $g_{1'}$, g_2, and $g_{2'}$ since all these signals coalesced simultaneously to give one broad signal at 253 K. This situation would arise if processes 1 and 2 in **2**·4PF_6 have similar activation energy barriers. Also, it should be noted that the differences in the separations between exchanging α-bipyridinium proton signals is small (< 40 Hz).

[33] P. R. Ashton, M. Grognuz, A. M. Z. Slawin, J. F. Stoddart, D. J. Williams, *Tetrahedron Lett.* **1991**, *32*, 6235–6238.

[34] a) We have found that simple indoles, such as 2-methylindole and 2-methyl-3-[(2-hydroxy)ethyl]-5-methoxyindole, form strongly colored charge-transfer complexes (λ_{max} at 485 nm and 535 nm, respectively) with cyclobis(paraquat-*p*-phenylene) in organic solvents such as MeCN. In the case of 2-methyl-3-[2-hy-

0947-6539/97/0307-1134 $ 17.50+.50/0

droxyethyl]-5-methoxyindole, high-field ^{1}H NMR spectroscopic studies indicate that the indole nucleus has its long "axis" directed perpendicular to the directions of the N–N vectors in the tetracationic macrocycle.

[35] T. T. Goodnow, A. E. Kaifer, M. V. Reddington, J. F. Stoddart, *J. Am. Chem. Soc.* **1991**, *113*, 4335–4337. See also: A. Mirzoian, A. E. Kaifer, *J. Org. Chem.* **1995**, *60*, 8093–8095.

[36] a) B. Robinson, *Chem. Rev.* **1963**, *63*, 373–401 and **1969**, *69*, 227–250; b) R. J. Sundberg, in *The Chemistry of Indoles*, Academic Press, New York, **1970**; c) B. Robinson, in *The Fischer Indole Synthesis*, Wiley, New York, **1982**; d) D. Zhao, D. L. Hughes, D. R. Bender, A. M. DeMarco, P. J. Reider, *J. Org. Chem.* **1991**, *56*, 3001–3006.

[37] A similar process has also been observed in the other molecular shuttles discussed in this paper.

[38] The first and second oxidation potentials of TTF are approximately 0.3 and 0.7 V, respectively, vs SCE (F. Wudl, M. L. Kaplan, E. J. Hufnagel, E. W. Southwick, *J. Org. Chem.* **1974**, *39*, 3608–3609).

[39] Originally, in a communication (D. Philp, A. M. Z. Slawin, N. Spencer, J. F. Stoddart, D. J. Williams, *J. Chem. Soc. Chem. Commun.* **1991**, 1584–1586) on the complexation of TTF by cyclobis(paraquat-*p*-phenylene)tetrakis-(hexafluorophosphate), we reported a K_a value of 51 M^{-1} in MeCN for the 1:1 complex. Subsequently, Professor M. R. Bryce (University of Durham) informed us that this K_a value was in error. After numerous experiments had been carried out in both laboratories, we reached the same conclusion, that is, that the K_a value in MeCN at 25 °C is ca. 8000 M^{-1} while in Me_2CO at 25 °C it is ca. 2600 M^{-1}. We thank Professor Bryce for bringing this error to our attention.

[40] The results of the spectrophotometric titration were evaluated by the computer-assisted nonlinear least-square curve-fitting (*UltraFit*, Biosoft, Cambridge, **1992**) of the experimental data of titration at 25 °C in CH_3CN, which gave a K_a value of $8030 \pm 535\ M^{-1}$ ($-\Delta G^\circ = 5.32 \pm 0.04$ kcal mol^{-1}) for the 1:1 complex formed between [BBIPYBIXYCY][PF_6]$_4$ and TTF.

[41] The results obtained by the dilution method, based on ^{1}H NMR chemical shifts (H. M. Colquhoun, E. P. Goodings, J. M. Maud, J. F. Stoddart, J. B. Wolstenholme, D. J. Williams, *J. Chem. Soc. Perkin Trans. 2* **1985**, 607–624) were evaluated by the computer-assisted nonlinear least-square curve-fitting of the experimental data recorded at 25 °C in CH_3CN which gave a value for K_a of $7190 \pm 970\ M^{-1}$ ($-\Delta G^\circ = 5.26 \pm 0.07$ kcal mol^{-1}) for the 1:1 complex formed between [BBIPYBIXYCY][PF_6]$_4$ and TTF.

[42] M. Nishio, Y. Umezawa, M. Hirota, Y. Takeuchi, *Tetrahedron* **1995**, *51*, 8665–8701 and references cited therein.

[43] The related species, bis(propylenedithio)TTF, has been prepared and studied, especially in the context of organic metals (M. Mizuno, A. F. Garito, M. P. Cava, *J. Chem. Soc. Chem. Commun.* **1978**, 18–19). An asymmetrical TTF derivative containing the 2-hydroxypropylenedithio moiety has also been reported recently (M. R. Bryce, G. J. Marshallsay, *Tetrahedron Lett.* **1991**, *32*, 6033–6036). However, in view of the difficulties involved in alkylating the secondary hydroxyl function in derivatives of this type, as well as the limited solubility of lower molecular weight TTF derivatives in many organic solvents, we decided to employ a different synthetic approach whereby the polyether-containing portions of the dumbbell-shaped component **1** are constructed prior to formation of the 4,5-dithio-1,3-dithiol-2-thione moiety. By forming the TTF nucleus in the final step of the synthesis of **1**, we also avoided possible complications associated with the instability of the dithio-TTF unit to a wide range of different reaction conditions. The TTF nucleus has been functionalized successfully with fused crown ether units. See, for example: a) B. Girmay, J. D. Kilburn, A. E. Underhill, K. S. Varma, M. B. Hursthouse, M. E. Harman, J. Becher, G. J. Bojesen, *J. Chem. Soc. Chem. Commun.* **1989**, 1406–1409; b) J. Becher, T. K. Hansen, N. Malhotra, G. Bojesen, S. Bowadt, K. S. Varma, B. Girmay, J. D. Kilburn, A. E. Underhill, *J. Chem. Soc. Perkin Trans. 1* **1990**, 175–177; c) B. Girmay, A. E. Underhill, J. D. Kilburn, T. K. Hansen, J. Becher, K. S. Varma, P. Roepstorff, *J. Chem. Soc. Perkin Trans. 1* **1992**, 383–385. Some extensive reviews concerning TTF and its derivatives have appeared in the literature. See, for example: a) A. Krief, *Tetrahedron* **1986**, *42*, 1209–1252; b) G. Schukat, A. M. Richter, E. Fanghänel, *Sulfur Reports* **1987**, *7*, 155–240. For other catenanes and rotaxanes incorporating TTF, see: a) Z.-T. Li, P. C. Stein, N. Svenstrup, K. H. Lund, J. Becher, *Angew. Chem. Int. Ed. Engl.* **1995**, *34*, 2524–2528; b) Z.-T. Li, P. C. Stein, J. Becher, D. Jensen, P. Mørk, N. Svenstrup, *Chem. Eur. J.* **1996**, *2*, 624–633; c) Z.-T. Li, J. Becher, *Chem. Commun.* **1996**, 639–640.

[44] P. E. Verkade, J. D. Van Roon, *Rec. Trav. Chim. Pays-Bas* **1942**, *61*, 831–841.

[45] a) G. Steimecke, H. J. Sieler, R. Kirmse, E. Hoyer, *E. Phosphorus Sulfur* **1979**, *7*, 49–55; b) K. S. Varma, A. Bury, N. J. Harris, A. E. Underhill, *Synthesis* **1987**, 837–838.

[46] FAB mass spectrometry was used to characterize **4**·4PF_6. Evident in the FABMS were peaks at *m/z* 2836, 2690, and 2545, corresponding to the loss of one, two, and three counterions, repectively, from the molecular assembly.

[47] The exchange method, where values of k were obtained (J. Sandström, in *Dynamic NMR Spectroscopy*, Academic Press, London, **1982**, Chapter 6) from the approximate expression $k = \pi(\Delta\nu)$, where $\Delta\nu$ is the difference (in Hertz) between the line width at a suitable temperature, T, where exchange of sites is occurring, and the line width in the absence of exchange. The Eyring equation was used to calculate ΔG^+ at T.

[48] a) M. J. Kamlet, J. L. Abboud, R. W. Taft, *J. Am. Chem. Soc.* **1977**, *99*, 6027–6038; b) M. J. Kamlet, J. L. Abboud, R. W. Taft, *ibid.* **1977**, *99*, 8325–8327; c) J. L. Abboud, M. J. Kamlet, R. W. Taft, *Progr. Phys. Org. Chem.* **1981**, *13*, 485–523.

[49] R. A. Bissell, E. Córdova, A. E. Kaifer, J. F. Stoddart, *Nature (London)*, **1994**, 369, 133–137.

[50] R. S. Nicholson, I. Shain, *Anal. Chem.* **1964**, 36, 706–723.

[51] R. L. Myers, I. Shain, *Anal. Chem.* **1969**, 41, 980.

[52] D. E. Richardson, H. Taube, *Inorg. Chem.* **1981**, 20, 1278–1285.

[53] E. Co'rdova, R. A. Bissell, A. E. Kaifer, *J. Org. Chem.* **1995**, 60, 1033–1038.

[54] J. C. Medina, T. T. Goodnow, M. T. Rojas, J. L. Atwood, B. C. Lynn, A. E. Kaifer, G. W. Gokel, *J. Am. Chem. Soc.* **1992**, 114, 10583–10595.

[55] D. D. Perrin, W. L. Armarego, *Purification of Laboratory Chemicals*, 3rd ed., Pergamon, New York, **1988**.

[56] S. C. Gupta, F. A. Kummerow, *J. Org. Chem.* **1959**, *24*, 409–415.

[57] H. S. Freeman, S.-D. Kim, R. D. Gilbert, R. McGregor, *Dyes Pigm.* **1991**, *17*, 83–100.